Republic of Iraq

Ministry of Higher Education and Scientific Research

University of Babylon

College of Education for Pure Sciences

Department of Physics

Investigating the effect of (ZnSe) Semiconductor Nanomaterial on the Linear and nonlinear Properties of (PMMA/PS) Polymer blend

A Thesis

Submitted to the Council of the College of Education for Pure Sciences of University of Babylon in Partial Fulfillment of the Requirements for the Degree of Master in Education / Physics

By

Ibtisam Hamzah Radhi Abdul Hussein

B. Sc. in Physics

(University of Babylon, 2004)

Supervised by

Prof. Dr. Zaid Abdul Zahra Hasan

2023 A.D **1445 A.H.**

نَرْفَعُ دَرَجَاتٍ مَّن نَّشَاءُ وَفَوْقَ كُلِّ

ذِي عِلْمٍ عَلِيمٌ ﴿٧٦﴾

صدق الله العظيم

سورة يوسف (الآية٧٦)

Dedication

I dedicate this work to Allah who always give me strength, knowledge, and wisdom in everything I do.

I dedicate this work to my husband and family, who encouraged and supported me throughout the study period

Ibtisam

Acknowledgments

I would like to express my deep gratitude and appreciation to my supervisor, Prof. Dr. Zaid Abdul Zahra Hasan for his guidance, suggestion, and encouragement throughout the research work, without him, this thesis would have been impossible.

Finally, I would like to thank all members of my family for their help and encouragements and my husband and my family and everyone who helped me during the preparation of this thesis.

Ibtisam

Supervisor's Certification

I certify that this Thesis entitled **" Investigating the effect of (ZnSe) Semiconductor Nanomaterial on the Liner and nonliner Properties of (PMMA/PS) Polymer blend "** is prepared by the student (**Ibtisam Hamzah Radhi Abdul Hussein**) under supervision at the College of Education for Pure Sciences, University of Babylon as partial fulfillment of the requirement for the degree Master of education / physics.

Signature:

Name: **Dr. Zaid Abdul Zahra Hasan**

Title: Professor

Date: / / 2023

Head of the Department Certificate

In view of the available recommendations, I forward this Thesis for debate by the examining committee.

Signature:

Name: **Dr. Khalid Haneen Abas**

Title: Professor

(Head of Physics Department)

Date: / / 2023

Summary

In this study, the Poly (methyl methacrylate)/Polystyrene/Zinc selenide (PS/PMMA/ZnSe) nanocomposites films has been prepared by using casting method with different weight percentage of (ZnSe) nanoparticles (1, 3 and 5) wt.%. The structural, linear and nonlinear optical properties of (PS/PMMA/ZnSe) nanocomposites films have been investigated.

The structural properties include optical microscope (OM) images and Fourier transformation infrared (FTIR). The optical microscope images show that ZnSe nanoparticles form relatively large size aggregates at ratio of doping of (5) wt.%. FTIR spectra of the (PS/PMMA/ZnSe) show a shift in some bands and change in the intensities of other bands comparing with pure (PS/PMMA) polymer. However, they do not include any new bands in comparison with the pure (PS/PMMA). This indicates that is no interaction between the polymers and the added nanoparticles. The optical properties showed that the absorbance, absorption coefficient, refractive index, extinction coefficient, dielectric constant (real, imaginary) and optical conductivity of (PS/PMMA/ZnSe) nanocomposites films increased with the increasing of the concentrations of the (ZnSe) nanoparticles. The transmittance and the energy gap for indirect transition (allowed, forbidden) between (3.8-2.8) eV decreased with the increasing of the concentrations of (ZnSe) nanoparticles.

The absolute value of the nonlinear refractive index and the nonlinear absorption coefficient increased with increasing concentration of ZnSe nanoparticles.

List of Content

List of Table

List of Figures

List of Symbol and Abbreviation

Symbol	Definition
0-D	Zero-dimension
1-D	One-dimension
2-D	Two-dimension
3-D	Three-dimension
PMMA	Poly(methyl methacrylate)
PS	Polystyrene
ZnSe	Zinc selenide
FT-IR	Fourier transform-infrared
hν	Energy of photon
E_g	Energy gap
h	Plank constant
C.B	Conductive bottom
V.B	Valence band
n	Refractive index
k_o	Extinction coefficient
ε_r	Real dielectric constant
ε_i	Imaginary dielectric constant
R	Reflectance
λ	Incident radiation wavelength
A	Absorbance
t	Thickness of sample
T	Transmittance
σ_{op}	Optical conductivity

Symbol	Definition
$\Delta\boldsymbol{\phi_0}$	The nonlinear phase shift
$\boldsymbol{L_{eff}}$	The effective length of the sample
$\mathbf{P_{peak}}$	The peak power
$\mathbf{\Delta t}$	The pulse duration
$\mathbf{Z}$	The sample position at the minimum transmittance
$\boldsymbol{Z_0}$	The diffraction length
$\mathbf{T(z)}$	The minimum transmittance
$\boldsymbol{\beta}$	The nonlinear absorption coefficient

Chapter One

Introduction and Literature Review

1.1 Introduction

Polymers are defined as macromolecules composed of one or more chemical units (monomers) that are repeated throughout a chain. Polymers are of profound interest to society and are replacing metals in diverse fields of life, which can be further modified according to modern applications [1]. They are more desirable than traditional materials in areas such as packaging, construction, and medical applications. The processing of polymeric materials depends on applied heat and pressure etc. [2].

Today, it is possible to create polymers from different elements with almost any quality desired in an end product. Some polymers are similar to existing conventional materials but with greater economic values, some represent significant improvements over existing materials, and some can only be described as unique materials with characteristics unlike any of the previously known to man. Polymer materials can be produced in the form of solid plastics, fibers, elastomers, or foams [3]. They may be hard or soft or maybe films, coatings, or adhesives. They can be made porous or nonporous or can melt with heat or set with heat. The possibilities are almost endless and their applications fascinating [4].

The polymer compound is a one-phase rigid multi-phase compound with separate polymer matrices in two or three dimensions [5]. In addition, polymer compounds can be used as high-performance components, because the reinforcement properties differ considerably and are better than the matrix properties. Polymer composites have excellent mechanical strength and stiffness, and are corrosion resistant [6]. A particular feature of polymers is the possibility of linking together separate chains to form networks. Such cross-links can be introduced by copolymerizing a monofunctional monomer such as styrene with a dysfunctional monomer such as divinylbenzene [7]. Polymers, such as polymethyl methacrylate, have excellent attention in many applications because

of their unique properties: low density, ability to form intricate shapes, and low manufacturing cost [8].

1.2 Structure of Polymer

The physical characteristics of polymer materials depend not only on molecular weight and shape but also on the molecular structure. different types of polymer chains are shown in Figure (1.1) [9]:

1. Linear polymers: Van der Waals bonding between chains. Examples: polyethylene and nylon.
2. Branched polymers: chain packing efficiency is reduced compared to linear polymers - lower density.
3. Cross-linked polymers: chain is connected by covalent bonds. Often, it is achieved by adding atoms or molecules that form covalent links between chains. Many rubbers have this structure.
4. Network polymers: 3D networks made from trifunctional mers. Examples: epoxies and phenol-formaldehyde.

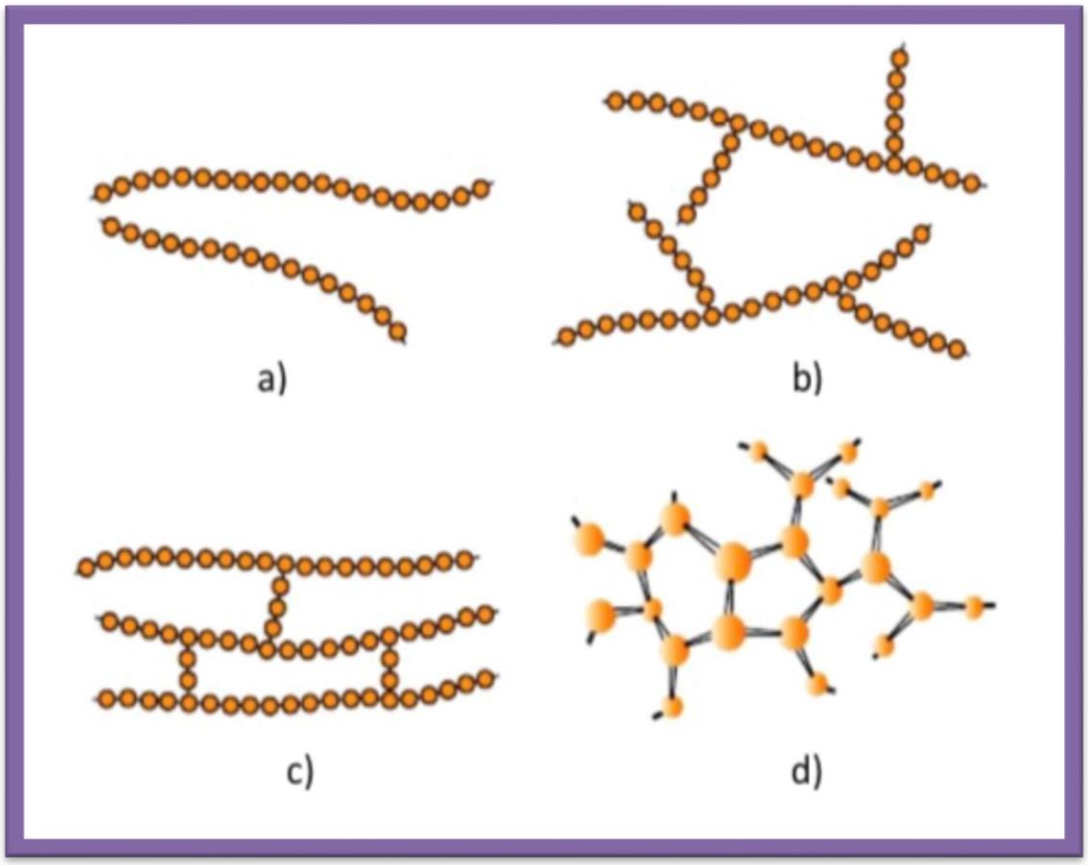

Fig. (1.1): Polymer Chains; a) Linear polymers, b) Branched polymers , c) Cross-linked , and d) Network polymers [9].

1.3 Nanomaterials

Nanotechnology is the creation and exploitation of nanomaterials with structural features between those of atoms and their bulk materials. Nanomaterials are the materials when the grain size of the individual building blocks between (1-100 nm) dimension, that is different from the bulk material and the characteristics that can be applied in most fields such as medical applications, biomedical applications, healthcare and life sciences, agricultures, food safety, security, energy production, energy storage, consumer goods, infrastructure, building and construction sector, and aerospace [10]. Over decades, the ability to tune surface morphologies and the structure of semiconductor materials with near atomic scale has led to further idealization of semiconductor structures: quantum wells, wires, and dots. These nanostructures have completely different density of electronic states predicted by simple particle in a box type models of quantum

mechanics [11]. Nanostructures of nanomaterials can be classified according to their basic dimensions (X, Y and Z) in space are shown in figure (1.3) [12]:

1. Zero-dimension (0-D) (represent for quantum dots or nanoparticles).
2. One-dimension (1-D) (indicate to nanowires, nanorods, nanofibres, nanobelts, and nanotubes).
3. Two-dimension (2-D) (refer to nanosheets, nanowalls and nanoplates).
4. Three-dimension (3-D) (represent to nanoflowers and other complex structures such as nanotetrapods).

1.4 Nanocomposites

Nanocomposite polymers are defined as homogenous or heterogeneous, two-phase systems that consists of polymers and fillers with at least one dimension within the nano-range (1-100) nm. The fillers can be Nano fibers, two-dimensional clay platelets, one dimensional nanotube, or three-dimensional spherical particles. Polymers are the most popular materials used in the manufacturing of nanocomposites such as thermoplastics, thermosets or elastomers [13].

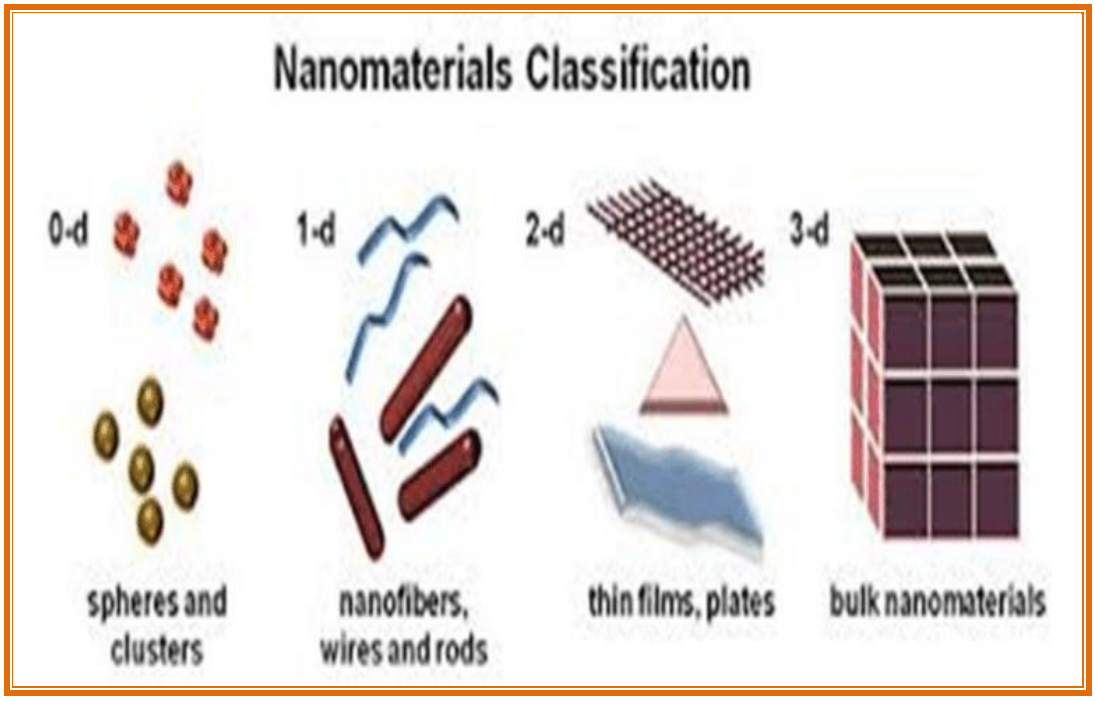

Fig. (1.2): Types of nanomaterial [12]

Over the past decades, polymer nanocomposites have drawn significant attention in both academia and industry, and they have become a crucial factor in the production of innovative advanced materials suitable for a range of uses, including electrical engineering [13]. Nano-composites are composed of synthetic and natural polymers, and nano materials, which refer to materials with nano sizes or are comprised from nano-sized building components [14]. The mechanical, electrical, thermal, electronic, and electro-chemical properties of nanocomposites can vary greatly from those of their component materials [15].

1.5 Literature Review

In (2013), P. P. Jeeju *et. al.* [16], prepared films of ZnO/PS/PMMA nanocomposites by using the spin coating technique to enhance the optical properties of these nanocomposites. They found that the ZnO/PS/PMMA nanocomposite films with 10 wt.% ZnO content exhibits shielding in the UV region and high transparency in the visible region. They found these results indicated optical limiting type nonlinearity in the films due to two-photon absorption. They also found that the minimum transmittance of around 0.25 has been observed in the ZnO/PS/PMMA nanocomposite films which is much lower compared to that in ZnO/PMMA and ZnO/PS nanocomposite films.

In (2014), N. G. Hamed and M. Rahem [17], studied the optical and electrical properties of Ag/PMMA composite, they prepared the samples as films with different concentrations by using the casting method. They found that there was a nonlinear proportion between the optical constants and the concentration ratio, which was attributed to their incompatibility. Also, they found an increase in the absorption spectra with an increase in the silver concentration in Ag/PMMA composites, they refered it to the increase in localized states. They also found the best conductivity was at a 9%Ag ratio and the lowest receptivity.

In (2015), S.K. Tripathi *et. al.* [18] studied investigation of non-linear of CdS/PS polymer nanocomposite. XRD spectra of CdS/PS nanocomposite reveals the cubic phase of CdS nanoparticles with average crystallite size 2.54 nm. The

vibrational band corresponding to CdS bond was observed at 406.57 cm^{-1} in FTIR spectra of CdS/PS nanocomposite along the typical styrene bonds. From the UV–vis spectra. In PL emission spectra, in addition to band-to-band transition emission, the green and yellow bands have been observed due to the interstitial sulfur and cadmium defect states respectively. Z-scan technique was utilized to study the non-linear optical properties of the CdS/PS nano- composite. The value of non-linear absorption coefficient (β) and non-linear refractive index(n_2) were calculated.

In (2016), Aya H. Makki *et. al*. [19] studied the effect of ZnO dopant on the nonlinear optical behavior of TiO_2-PMMA nanocomposites films were studied. TiO_2-PMMA Nano composites films were pre pared using solution casting method then doped with different amounts of ZnO nanoparticles. Z-Scan measurements were performed to obtain the nonlinear optical response of these samples at 1064nm using CW Nd- YAG laser. The addition of ZnO nanoparticle into the Nano composites showed a great enhancement in the nonlinear optical response and decreasing in limiting threshold (10 mW) as the dopant's concentration increased.

In (2017), M. T. Ramesan *et. al*. [20], prepared the nanocomposites of poly (vinyl alcohol) - poly (vinyl pyrrolidone) / silver-doped zinc oxide (Ag-doped ZnO). The intermolecular interaction between the polar component of the mix and the metal oxide nanoparticles was shown by the FT-IR and UV spectra. The structurally ordered arrangements of nanoparticles inside the polymer matrix were determined using SEM and XRD patterns. The electrical characteristics of the composites, such as AC conductivity and dielectric properties, were shown to rise with an increase in nanoparticle content up to a particular concentration (5 wt. percent), after which the value decreased.

In(2018), DongxiangLi and WeihongLin [21], In this letter, the nanocomposites of gold nanorods and ormosil gel glass were prepared by a solvent-assisted dispersing process and characterized by UV–vis spectra, TEM, XRD and optical limiting measurement. The results showed that these

gold/ormosil nanocomposites could preserve optical limiting property of gold nanorods and had enhanced thermostability due to thermostable silica matrix. Such nanocomposite material of metal-doped gel glass matrix could be considered as a promising candidate for optical limiter against tunable laser.

In (2019), L. Gahramanli *et. al*. [22] studied the surface modification of ZnSe crystal was carried out by silver ions. After ion exchange of crystal, on the surface area was formed Ag_2Se compound from XRD results. As seen from SEM image, the surface area was modified by the affect of heating with silver ions in the Muffle oven. Porosities were formed on the surface area and ZnSe were transformed to Ag_2Se. After ion exchange of crystal, the band gap value decreases 1.1eV.

In (2020), A. M. Alsaad *et. al*. [23], studied PMMA-PS/ZnO nanocomposites by using dip-coating technique. UV-Vis spectrophotometer measurements showed that the transmittance for PMMA-PS/ZnO thin films had strong absorption in UV region ($\lambda \leq 300\ nm$) and high values of transmittance in the visible region. they found that the transmittance values increased gradually upon introducing the ZnO NPs in the films and exhibit a maximum value of 85% for PMMA-PS/10% NPs. The structure and the morphology of the obtained doped polymers using EDAX mapping and SEM micrographs. their results indicated that Zn atoms was distributed uniformly in the structure. As-prepared Transparent PMMA-PS/ZnO Polymeric Nanocomposite Films were of great quality and could be used for several important optical applications.

In (2021), Q. M. Al-Bataineh *et. al.* [24], studied optically characterize pure PMMA and PMMA incorporated with metal oxides nanoparticles (MO NPs) such as ZnO, CuO, TiO_2 and SiO_2 NPs with weight concentration of 10% using dip-coating technique. SEM images of MO NPs show that all NPs had nearly an average size of around 50 nm. The optical parameters such as, optical parameters (n and k), optoelectronics properties, dispersion, band-gap energy and band structure of as-prepared nanocomposite thin films were determined by analyzing the transmittance and reflectance spectra. Mainly, optical band-gap energy (E_g)

and the thickness of thin films were evaluated to a high degree of accuracy by utilizing Q-functional derived using a mathematical model recently published. The Eg value of un-doped PMMA thin films is found to be 4.273 eV. This value decreased as pre-selected MO NPs were introduced into thin films. The FTIR technique was employed to elucidate the vibrational bands of the nanocomposites and the intermolecular bonding between PMMA matrix and the MOs NPs.

In 2022, M. H. Noory and Z. A. Hasan [25], prepared methyl blue dye doped with silicon oxide (SiO_2) nanoparticles with different weight ratios (1, 3 and 5) % by a dropping and swiping method on glass slides at room temperature and atmospheric pressure to obtain films of varying thicknesses (15 -25) μm. It was found that the alloy plays a role in improving the optical properties well, as good refractive values were obtained that are useful for use in applications that need large refractive indexes. It was also found that the optical transmittance decreases with increasing the doping and thus increasing the absorbance, reaching the highest peak in the visible field around 600 nm. The closed aperture Z-scan results for all cases showed high nonlinear optical properties, and negative self-defocusing. The Z-Scan scan results with a three-state open aperture (MBD: SiO_2) nanocomposites gave a two-photon absorption, while pure (MBD) without SiO_2 nanoparticles gave a saturated absorption.

1.6 The Aims of The Study

Synthesis (PMMA/PS/ZnSe) nanocomposites films and study their linear and nonlinear optical properties.

Chapter Two

Theoretical Consideration

2.1 Introduction

This chapter presents the main theoretical concepts and basic definitions that are adopted in this work.

2.2 Structural and Morphological Properties

2.2.1 Optical microscope

A compound optical microscope is an optical tool that magnifies an object (or specimen) and projects it onto the retina of the eye or onto an imaging device using visible light. The term "compound" refers to how two lenses, the objective lens and the eyepiece (or ocular), work together to generate the image's final magnification [26]. Both diffracted (rays that interact with the specimen) and non-diffracted (rays that pass through the specimen without deviating) rays are gathered by the objective lens in most kinds of transmitted light microscopy and contribute to picture generation [27].

2.2.2 Fourier Transforms Infrared (FTIR) Spectroscopy

The Fourier Transform Infrared (FTIR) Spectroscopy is a non-destructive chemical characterization method. This spectral region is classified into three regions: far-infrared, near-infrared and, mid-infrared which are between (4~400 cm^{-1}), between (400~4,000cm^{-1}) and lastly, between (4,000~14,000 cm^{-1}), respectively [28]. FTIR spectroscopy is a vibrational spectroscopic method that can be used for the optical study of molecular shifts. The allowable existence of this technology relies on the identification of vibration in the sample by the chemical functional group [29-30]. Wherever an interaction takes place between infrared light and matter, the chemical bonds will stretch. [31]. Thus, a molecule is only absorbed at frequencies corresponding to its molecular vibration modes in the region of the electromagnetic spectrum between the visible (red) and the short (microwave) waves when exposed to radiation emitted by the thermal emission of a hot source (the source of IR energy) [32].

2.3 Optical Properties

The optical absorption spectroscopy technique is a very efficient method for examining electronic changes induced by light. Additionally, they investigate the energy gap and band structure of crystalline and amorphous materials theoretically. According to this idea, photons with an energy level greater than the band gap energy are collected by the absorption and transition of ultraviolet and visible light [33].

In the past few years, more people have been looking for optical qualities because they are used in integrated optics, like optical data storage and optical information. A lot of attention has also been paid to research on the optical and electrical properties of polymers because they are used in related devices [34]. Electrical conduction in polymers was examined with a view to understanding the characteristic features of the load transport prevailing in these materials, whereas optical properties are developed to enhance reflective and anti-reflective interference and polarization properties [35].

2.3.1 Absorbance (A)

It is the phenomenon in which radiation relinquishes a portion or the entirety of its energy to the medium in which it traverses. The reduction of the overall energy of the radiation is known as attenuation. In the event that liquid materials are involved, the absorbing incident photons exhibit a direct correlation with the concentration of the absorbing molecules of the sample. The absorbance of the medium can be expressed mathematically as [36].

$$A = log_{10}\left(\frac{I_0}{I}\right) = \varepsilon \ell C \qquad (2.1)$$

where, I: is the intensity of rays at wavelength (λ) passing through the sample (transmitting intensity), I_0: is the incident intensity, C: is the concentration of the absorbing material, ε: is the molar extinction coefficient and its units (M^{-1} cm^{-1}), and ℓ: is the thickness of the material through which the incident ray passes

2.3.2 Transmittance (T_r)

The intensity of transmitted rays from the film (I) over the intensity of incident rays on the film (I_0) is called the transmittance (T) and can be obtained as follows [37].

$$T = I/I_0 \quad (2.2)$$

2.3.3 The Absorption Coefficient (α)

The absorption coefficient refers to the decrease in the incoming radiation per unit length of the medium along the direction of wave propagation [38]. It depends on the photon energy (hυ). Photon energy created by Planck's relationship [36]:

$$E = h\nu = \frac{hc}{\lambda} \quad (2.3)$$

where: c: is the light's velocity and λ: is the light's wavelength. The absorption coefficient can be calculated from Lambert's law as [26]:

$$I = I_o e^{-\alpha d} \quad (2.4)$$

where: (d) is the thickness of the sample.

$$\alpha\, d = 2.303\, logs\, (I_O / I) \quad (2.5)$$

But $A = log\, (I_O / I)$

$$\alpha\, d = 2.303 \times A \quad (2.6)$$

Then:

$$\alpha = (2.303 \times A) / d \quad (2.7)$$

where: (A) is the absorbance of the material.

2.3.4 Fundamental Absorption Edge

The fundamental absorption edge can be defined as the rapid increasing in absorbance when absorbed energy radiation is almost equal to the band energy gap; therefore [40], the fundamental absorption edge represents the less difference in the energy between the up point in the valance band to the bottom point in conduction band [41].

2.3.5 Absorption Regions

Absorption regions can be classified into three regions, as seen in Figure (2.1):

A) High Absorption Region

In this area, the absorption coefficient is about ($\alpha \geq 10^4$ cm^{-1}) [42].

B) Exponential Region

The value of absorption coefficient (α) is equal to ($1\ cm^{-1} < \alpha < 10^4\ cm^{-1}$). It indicates the transition from the extended level at the top of the valence band towards the localized level at the conductive band and vice versa, from the local level towards the extended level at the bottom from conductive band [43,44].

C) Low Absorption Region

The absorption coefficient (α) in this region is very small, it is about ($\alpha<1cm^{-1}$). The transition happens in this region because of state density inside space motion results from faults structural [45,46].

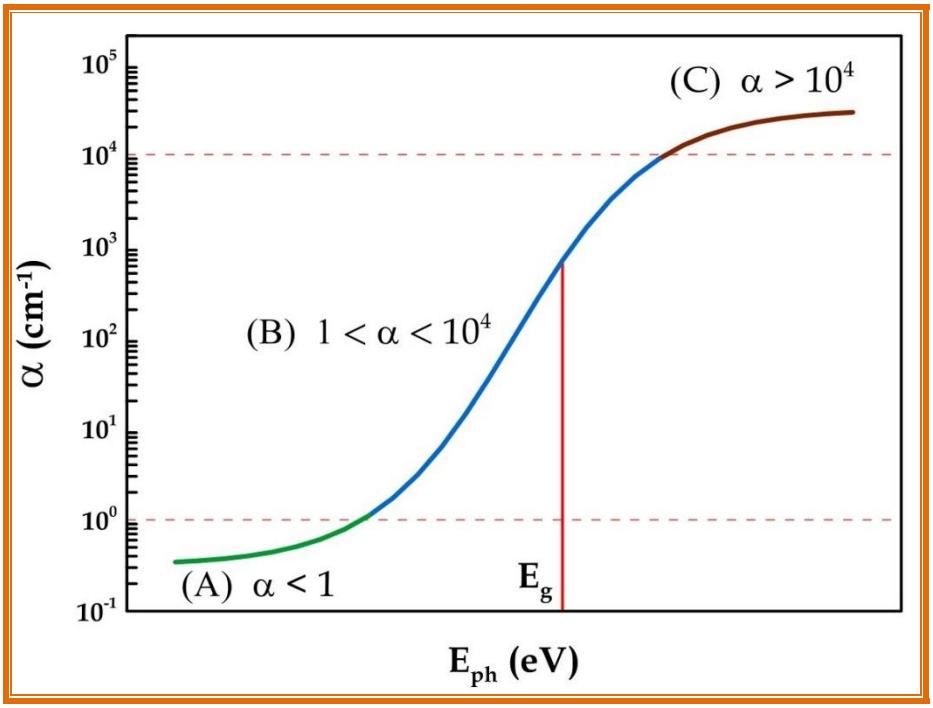

Fig. (2.1): The Absorption Regions [47].

2.3.6 Electronic Transitions

The electronic transitions can be classified basically into two types:

2.3.6.1 Direct Transition

This transition occurs in semiconductors when the bottom of the conduction band (C.B.) is exactly over the top of the valence band (V.B.) indicating that they have the same wave vector value, i.e. $\Delta K=0$; absorption occurs in this state when ($h\upsilon = E_g^{opt}$). The conservation of energy and momentum was needed for this transition form [48]. Direct transitions are classified into two kinds:

A- Direct Allowed Transition

This transition happens from the top points in the valance band and the bottom point in the conduction band [49], as shown in Figure (2.2 A).

B- Direct Forbidden Transitions:

This transition happens from the near top points of the valance band and the bottom points of the conductive band, as shown in Figure (2.2 B).

The absorption coefficient for this transition type is given by [50]:

$$\alpha h\nu = B\left[h\nu - E_g^{opt}\right]^r \quad (2.8)$$

where: E_g^{opt}. the energy gap between direct transition.

B: constant depended on the type of material.

r: exponential constant, its value depended on the type of transition,

r =1/2 for the allowed direct transition.

r =3/2 for the forbidden direct transition.

2.3.6.2 Indirect Transitions

As for the electronic optical indirect transition, the bottom of the conduction band and the top of the valance band are in various regions of space (k). This type of transformation happens with the aid of the phonon to maintain the motion arising from variation in the electron wave vector. Two types of indirect transition exist, namely whenever the transition is between the top point of the valance band and the lower point of the conduction band, which is located in the various regions of the space (k) called indirect transition as shown in Figure (2.2 C): when these transitions happen between near points in the top of valance band and near points in the bottom of a conductive band called forbidden indirect transitions, as shown in Figure (2.2 D) [51]. As seen in Figure (2-2), the coefficient of absorption for a transition with phonon absorption can be obtained through the following equation:

$$\alpha h\nu = B\left[h\nu - E_g^{opt} \pm E_{ph}\right]^r \quad (2.9)$$

where (E_{ph}) is the energy of phonon. The value is (-) when the phonon is absorbed, whereas it is (+) in case the phonon is emitted. The value of (r) is (2) and (3) for the allowed and forbidden indirect transitions, respectively.

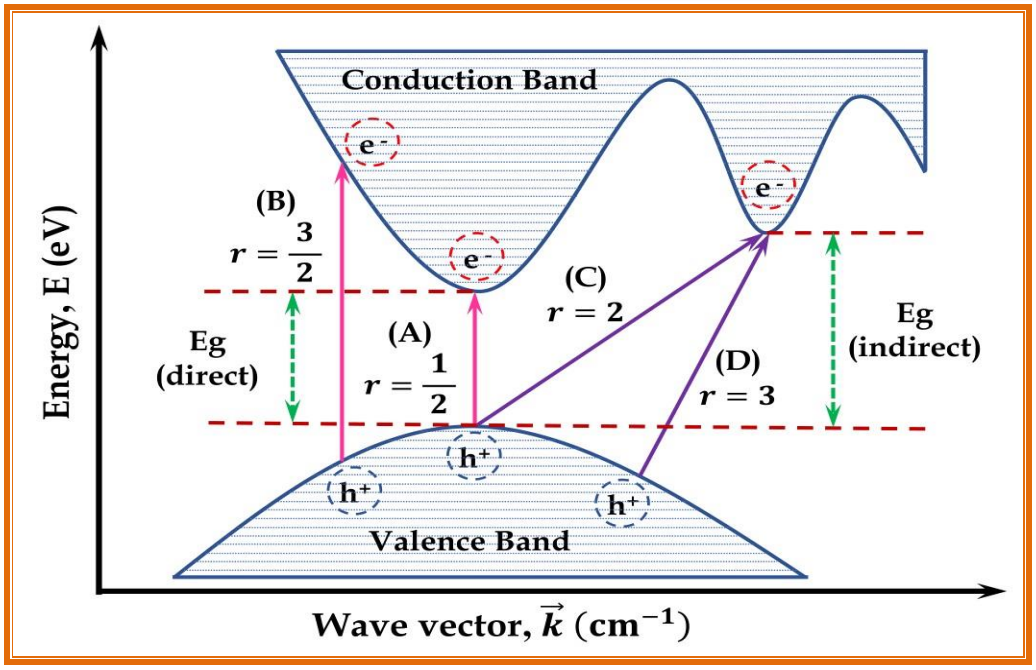

Fig. (2.2): The Electronic transitions types of (a) Allowed direct, (b) Forbidden direct transition, (c) Allowed indirect, and (d) Forbidden indirect transitions [52].

2.3.7 The Refractive Index (n)

It is the ratio of light speed in a vacuum to its speed in a medium. This index shows how far a matter is affected by electromagnetic waves. It can be expressed by the following equation [53]:

$$n = \frac{c}{v} \qquad (2.10)$$

where (n) is the refraction index, (c) is the light speed in a vacuum, and (v) is the light speed in the matter. The reflectance (R) was calculated from the transmission (T) and absorbance (A) values through the following equation [54]:

$$R + A + T = 1 \qquad (2.11)$$

The refractive index (n) can be calculated using following equation [55].

$$n = [4R/(R-1)^2 - k^2]^{1/2} + (R+1)/(R-1) \qquad (2.12)$$

2.3.8 Extinction Coefficient (k_o)

The extinction coefficient (K_o) presents the amount of attenuation of the electromagnetic wave that passes through a material. Its value is determined by

the density of the free electrons within the material and its structure, and expresses by the following relationship [56]:

$$k_0 = \alpha\lambda/4\pi \quad (2.13)$$

where (k_0) is the extinction coefficient, and (λ) is the wavelength of the incident light.

2.3.9 The Dielectric Constant (ε)

The dielectric constant serves as an indicator of the polarization capacity of a material. The real and imaginary components of the dielectric constants (ε_1 and ε_2) can be computed using the following equations [57]:

$$\varepsilon_1 = (n^2 - k^2) \quad (2.14)$$

$$\varepsilon_2 = (2nk) \quad (2.15)$$

2.3.10 The Optical Conductivity (σ)

The optical conductivity (σ) can be calculated by using the equation [58]:

$$\sigma = \alpha nc/4\pi \quad (2.16)$$

2.4 Nonlinear optical properties

The optical properties of materials are modified by high-intensity light such as a laser. The study of this phenomenon is called Nonlinear Optics. This phenomenon is observed in a wide variety of materials like dyes, polymers, semiconductors, nanomaterials, etc. [59]. After the invention of the first working laser by Theodore Maiman in 1960, Peter Franken et al demonstrated the first nonlinear optical phenomenon – second-harmonic generation in 1961. This has been considered the beginning of the study of nonlinear optics [60].

2.4.1. Nonlinear Absorption and Nonlinear Refraction

The main optical properties involved in the light-matter interaction are absorption, which is defined by the nonlinear absorption coefficient β, and

nonlinear refractive index n_2. These two parameters are depending on the electric field intensity of laser light [61]. When the material is irradiated, the energy of the absorbed photons makes it possible for the transition from the ground state to the excited state, and this represented a linear absorption. The further excitation may be possible due to the increasing of incoming photons (i.e., two photon absorption or multi photon absorption), this represents a type of nonlinear absorption [62].

There is also a change in the refractive index when a material is placed in a strong electric field. In fact, the index of refraction becomes dependent on the intensity of the electric field. At high intensity (I) of laser light, the refractive index is given by [63]:

$$n = n_0 + n_2 I \tag{2.17}$$

where, n_o: linear refractive index, n_2 is the nonlinear refractive coefficient related to the irradiance. The absorption of the material is also intensity dependent given by [64]:

$$\alpha = \alpha_0 + \beta I \tag{2.18}$$

where α_o, is the linear absorption coefficient, β is the nonlinear absorption coefficient related to the intensity. The coefficients n, and α are related to the intensity of laser.

2.4.2. Saturable Absorption

A nonlinear process that can be associated with real (rather than virtual) energy levels and population changes in those levels is that of saturable absorption [65]. This process occurred when the nonlinear absorption coefficient $\beta < 0$, which can appear when a strong light absorption between two levels causes saturation (bleaching) of the corresponding electronic transition. The two levels are involve surface resonance ground and excited state [66]. On the other hand, this is a process in which a material can be highly absorbing at a specific wavelength when a low-intensity beam is incident upon the material, yet an extremely intense beam

(at that same wavelength) will pass through the medium with little change in intensity [67].

2.4.3. Two-Photon Absorption

A nonlinear process that involves the transfer of energy to excited energy levels of the material [68]. This process occurred when the nonlinear absorption coefficient $\beta > 0$. This effect is shown in figure (2.3) [69].

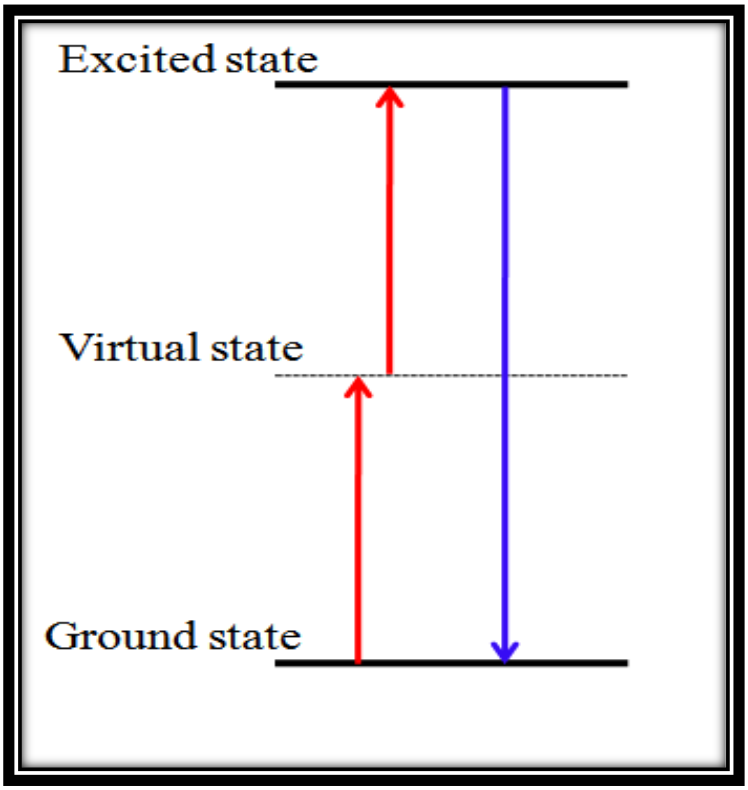

Fig. (2.3): Two-photon absorption [69].

2.4.4. Kerr Effect

A nonlinear interaction of light in a medium related to the nonlinear electronic polarization, which can be described as modifying the refractive index [70]. For high-intensity laser beams, the Kerr effect can create a local change in the refractive index that causes the laser material to act as a lens. This can result in self-focusing of laser beams [71].

2.4.5 Self-focusing and Self-defocusing

Self-Focusing (or Self-Defocusing): This occurs when a light beam of non-uniform intensity falls on a nonlinear medium. Since the nonlinear index follow the shape of the beam (for local effects without saturation), an index gradient is induced in the medium. For a positive nonlinearity, induces greater index, and hence, larger phase retardation on-axis than the wings result to focus the beam, negative nonlinearity induces the defocusing of the beam, as shown in figure (2.4) [72]. The NRI has generated significant scientific and technological interest. It has been utilized in or considered for a variety of the applications such as nonlinear spectroscopy, correcting (or finding) optical distortions, optical switching, optical logic gates, optical data processing, optical communications, optical limiting, passive laser mode-locking, waveguide switches and modulators [73].

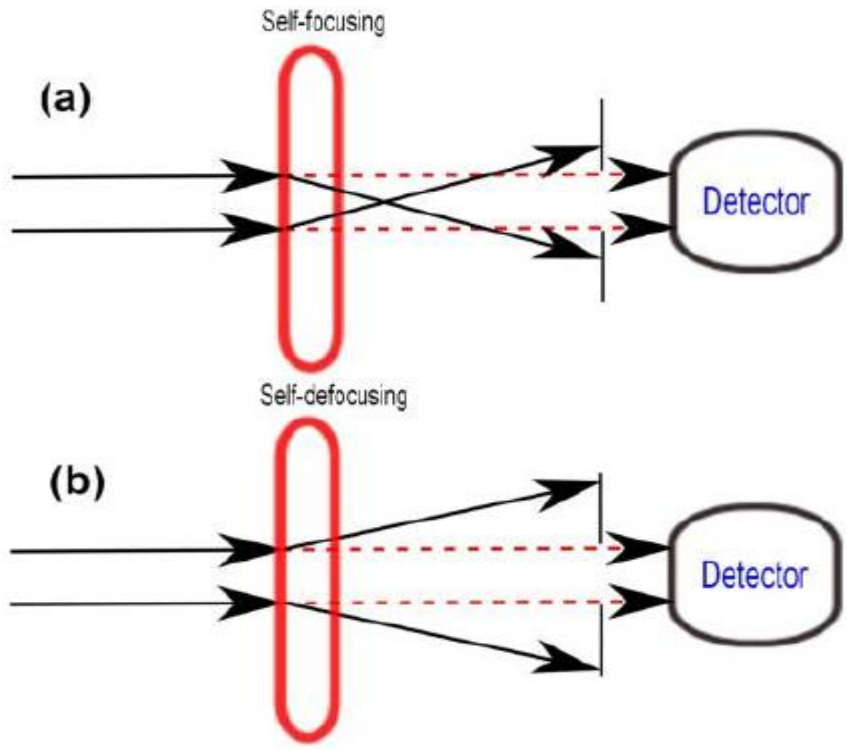

Figure 2.4 : self-focusing and self-defocusing of a Gaussian beam [73].

2.5 Z-Scan Technique and Nonlinear Optical Properties Measurements

Z-Scan technique is a simple and direct method to characterize both the nonlinear refraction and nonlinear absorption coefficients. It is based on a single beam method and it refers to the process of inserting a sample in a focused Gaussian beam and translating it along beam axis through a focal region. The wave front distortion from self-focusing or self-defocusing are results of the kerr nonlinearity [74]. The beam power propagating through a small aperture at far field varies with a sample position. Measuring the output power versus position sample allows to determine nonlinearity. There are two methods of Z-Scan, the closed-aperture and open-aperture system [75].

2.5.1 Closed-Aperture Z-Scan

A closed-aperture Z-Scan measures the change in power intensity of a beam, focused by lens (L) in figure (2.5). Photo-detector (PD) collects the light that passes through an axially centered aperture (A) in the far field. The change in on-axis intensity is caused by self-focusing or self-defocusing by the sample (S) as it travels through the beam waist [76].

A (TEM_{00}) Gaussian beam has the greatest intensity at the center and will create a change in index of refraction forming a lens in a nonlinear sample as shown in figure (2.5) [77]. This can be considered as a thin lens of variable focal length. Beginning far from the focus ($z<0$), the beam irradiance is low and nonlinear refraction is negligible. In this condition, the measured transmittance remains constant (i.e.,z-independent).As the sample approaches the beam focus (focal point of lens), irradiance increases, leading to self-lensing in the sample [78].

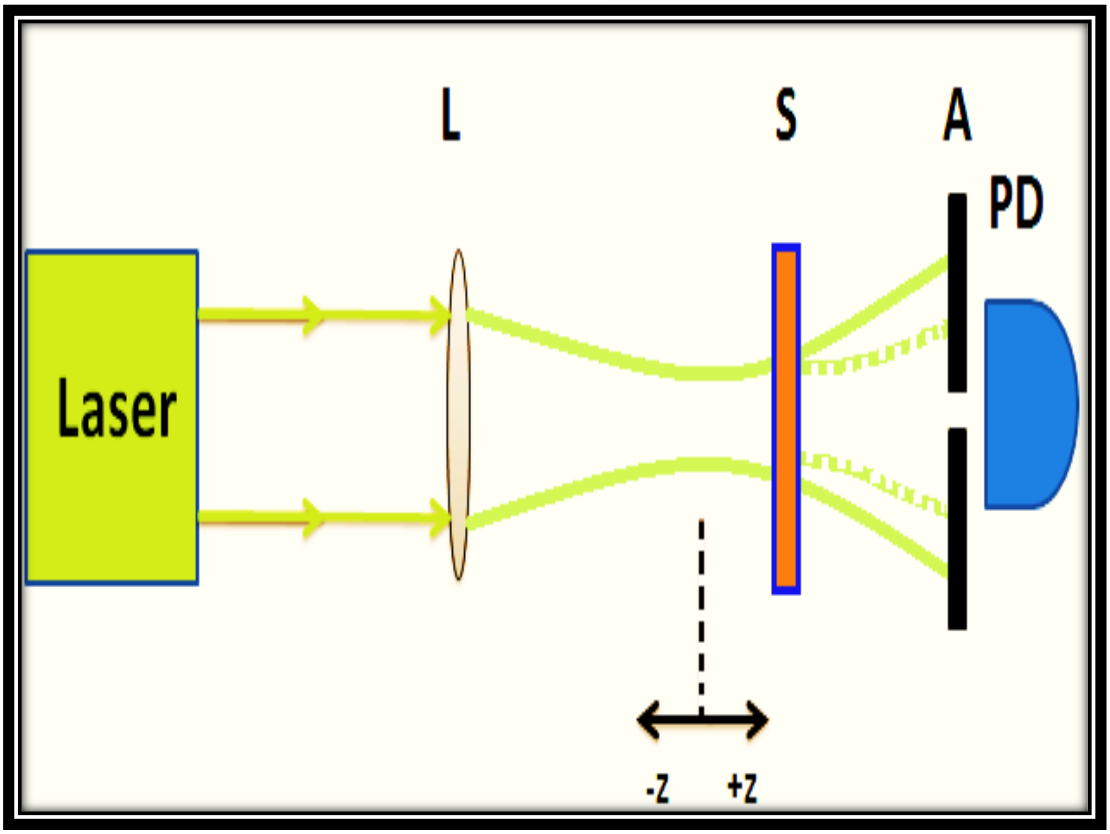

Fig. (2.5): Closed-Aperture Z-Scan [77].

A negative self-lens before the focal plane tend to collimate the beam on the aperture in the far field, increasing the transmittance measured at the iris position. After the focal plane, the same self-defocusing increases the beam divergence, leading to a widening of the beam at the aperture and thus reducing the measured transmittance [78].

Far from focus (z>0), again the nonlinear refraction is low resulting in a transmittance z-independent. A pre-focal transmittance maximum (peak), followed by a post-focal transmittance minimum (valley) is a Z- Scan signature of a negative nonlinearity [79]. An inverse Z-Scan curve (i.e., a valley followed by a peak) characterizes a positive nonlinearity. Figure (2.6) depicts these two situations [80].

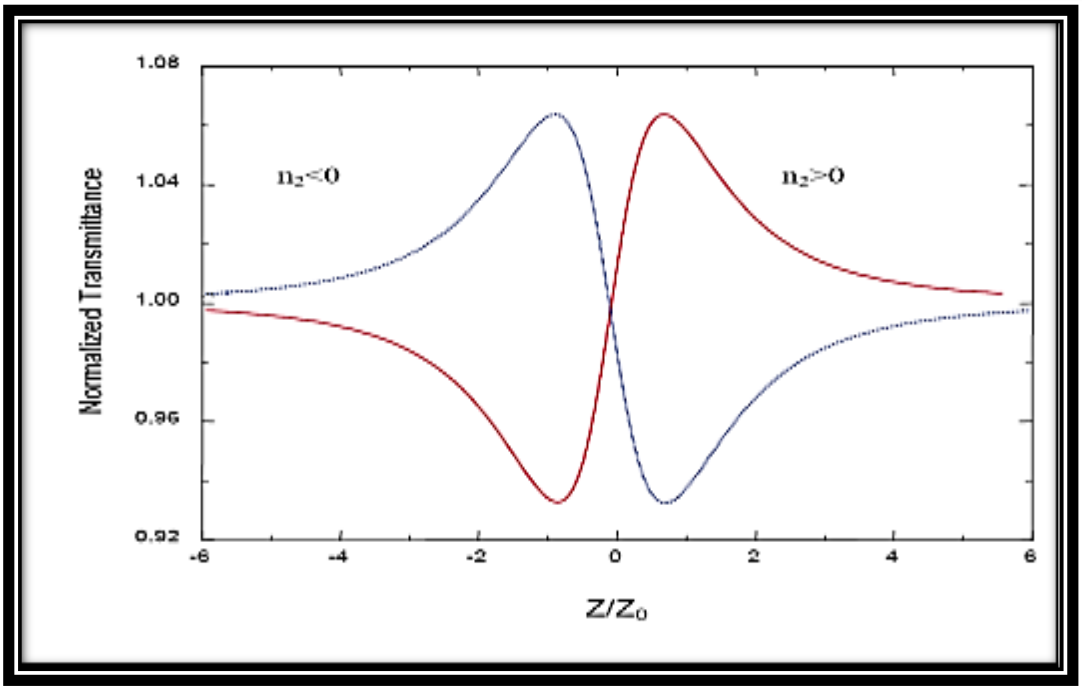

Fig. (2.6) : Calculated Z-Scan transmittance curves for a cubic nonlinearity [80].

The nonlinear refractive coefficient is calculated from the peak to valley difference of the normalized transmittance by the following formula [8 1]:

$$n_2 = \frac{\Delta\phi_0}{I_0\, L_{eff}\, k} \qquad (2.19)$$

Where, $k = 2\pi/\lambda$, is wave number , λ is the beam wavelength, I_0 is the intensity at the focal spot ,$\Delta\Phi_0$ is the nonlinear phase shift [82]:

$$\Delta T_{p-v} = 0.406|\Delta\phi_0| \qquad (2.20)$$

where ΔT_{p-v} is a difference between the normalized peak and valley transmittances, Leff is the effective length of the sample, determined from [83]:

$$L_{eff} = \frac{1-\exp(-\alpha_0\, L)}{\alpha_0} \qquad (2.21)$$

where L is the sample length, α_0 is linear absorption coefficient which is given as [84]:

$$\alpha = (2.303 \times A) / d \qquad (2.22)$$

where (d) is the thickness of sample and T being the transmittance.

The intensity at the focal spot is given by [85]:

$$I_0 = \frac{2P_{peak}}{\pi\, \omega_0^2} \qquad (2.23)$$

Is defined as the peak intensity within the sample at the focus, where ωo is the beam radius at the focal point.

2.5.2 Open-Aperture Z-Scan

An open-aperture Z-Scan measures the change in power intensity of a beam, focused by lens (L) in figure (2.7), in the far field at detector (PD), which captures the entire beam [86]. The change in power intensity is caused by nonlinear absorption in the sample S as it travels through the beam waist. In the focal plane where the intensity is the greatest, the largest nonlinear absorption is observed [87]. At the "tails" of the Z-Scan signature, where | z | >> zo, the beam intensity is too weak to elicit nonlinear effects. The higher order of multiphoton absorption present in the measurement depends on the wavelength of light and the energy levels of the sample. Clearly, even with nonlinear absorption, a Z-Scan with a fully open aperture is insensitive to nonlinear refraction (film sample approximation) [88].

The Z-Scan traces with no aperture are expected to be symmetric with respect to the focus (z=0) where they have a minimum transmittance (For example, multiphoton absorption) or maximum transmittance (For example, saturation of absorption) [89]. The coefficients of nonlinear absorption (β), can be easily calculated by using following equation [90]:

$$\beta = \frac{2\sqrt{2}\,\Delta T(z)}{I_0\, L_{eff}} \qquad (2.24)$$

where $\Delta T(z)$:is the difference between the sample transmittance at the linear regime and the minimum value of normalized transmittance at the focal point ,where (z=0), It should be clear that the transmittance versus sample position

graph of such an open aperture Z- Scan should be symmetric around the focus as shown in figure (2.8) [91] .

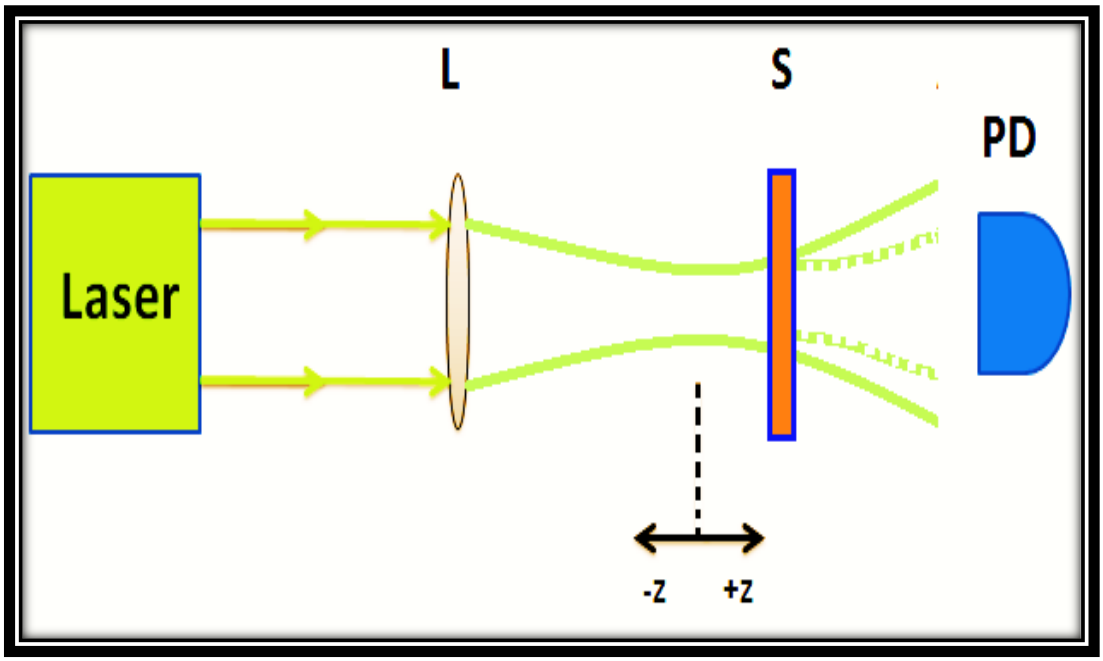

Fig. (2.7) : Open-aperture Z-Scan [86].

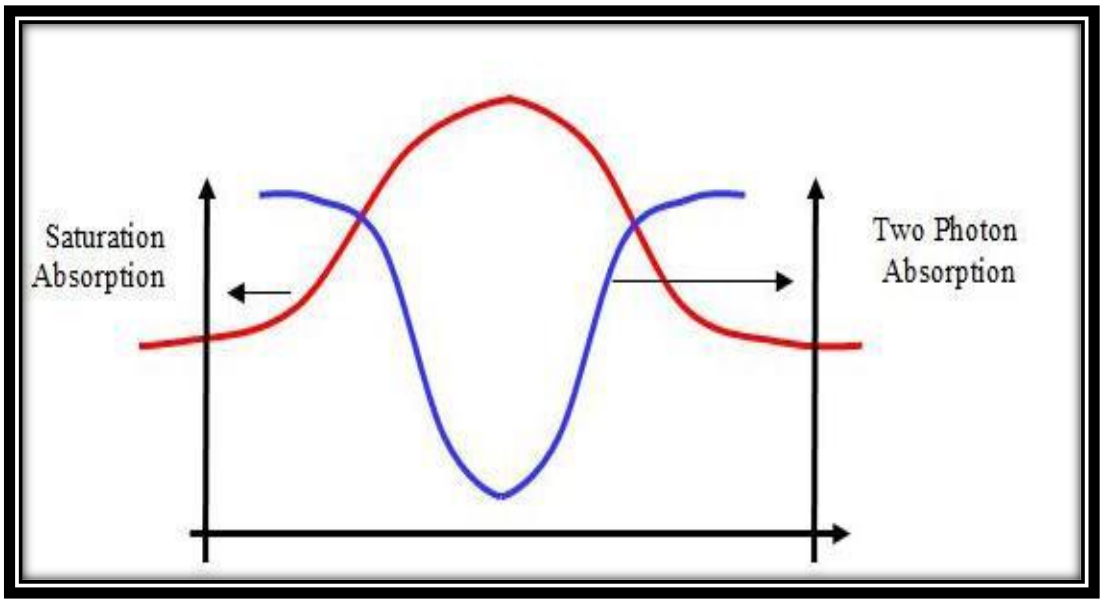

Fig. (2.8): Open aperture Z-Scan curve [91].

Chapter Three

Experimental Work

3.1 Introduction

This chapter discusses the processes involved in the preparation of samples, the use of instruments, and measurement methodologies. A general description of the materials Polystyrene (PS), Polymethyl methacrylate (PMMA) and zinc selenide (ZnSe). This study makes use of a variety of microscopy methods, including optical microscopy, Fourier Transform Infrared (FTIR), liner and non-liner optical properties measurements.

3.2 The Utilized Materials

3.2.1 Poly(methyl methacrylate) (PMMA)

Poly (methyl methacrylate) is one of the earliest and best-known polymers. It is a significant and fascinating polymer due to its appealing physical and optical features, which determine its wide applicability. PMMA is a non-biodegradable polymer with good transparency, mechanical strength, less weight, and chemical resistance. Thermoplastic material has a good tensile strength and hardness, and high rigidity. If it is polymerized between the float glass panels, it has a high shine on the surface [92]. Besides being polishable, it is weatherproof and resistant to weak acids and alkalis, non-polar solvents, fats, oils, and water without sacrificing its structural integrity. As a result of its outstanding light transmission and the fact that it can be colored to a high degree of saturation, (PMMA) is widely used in the lighting sector [93]. The PMMA (acrylic) polymer exhibits high levels of light transmission, making it an excellent choice for optical applications. PMMA enables lighter to travel through it than glass or other polymers, allowing 92 % of light to pass through. Table (3-1) shows the most important properties of PMMA polymer. These plastics can be easily thermoformed without any loss of visual clarity compared to polystyrene and polyethylene [94]. (PMMA) has been successfully utilized to freeze enzymes, build micro-locked devices, precipitate minerals, and freeze proteins and DNA [95]. Figure (3.1) shows the chemical structure of the PMMA polymers.

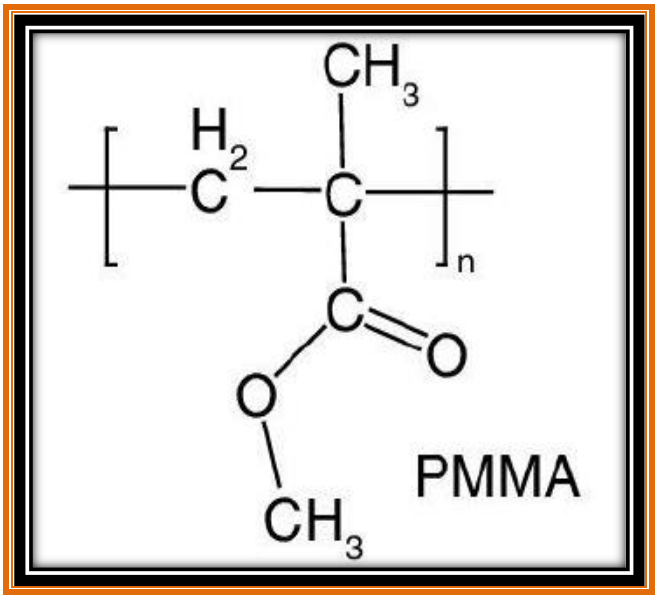

Fig. (3.1): Chemical Structure of PMMA [94].

Table (3.1) : The Most important Characteristics of PMMA [93].

Parameters	Description
Chemical formula	**$(C_5O_2H_8)_n$**
T_g (°C)	**106 °C**
Refractive index	**1.49**
Density	**1.2 g/cm^3**
Melting point	**160 °C**
Molecular weight Mw (gm/mol)	**100.116gm/mol**

3.2.2 Polystyrene (PS)

Polystyrene (PS) is a flexible plastic that is commonly used in several aspects of human life and industry due to its low cost, light weight, ease of fabrication, flexibility, thermal efficiency, durability, and moisture resistance [95]. However, polystyrene is exceptionally stable and difficult to degrade in the surroundings after disposal [96]. It is produced by the polymerization of styrene and is the most widely used plastic. At room temperature, the thermoplastic polymer is a solid but when heated above 100 °C it flows. It becomes rigid again when it cools down. Polystyrene is insoluble in water. Polystyrene is compound that is non-biodegradable with a couple of exceptions. It is easily dissolved by

many aromatic hydrocarbon solvents and chlorinated solvents. It is widely used in the food-service industry as rigid trays, containers, disposable eating plates, bowls, etc [97,98]. Figure (3.2) shows the chemical structure of the PS polymer's [99]. Table (3-2) explains some physical properties of PS [100,101].

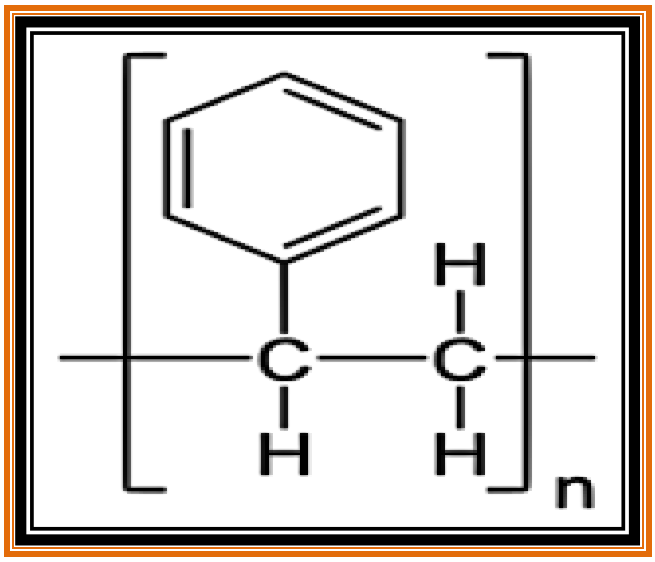

Fig. (3.2): The Chemical Structure of the PS [99].

Table (3.2): Physical Properties of PS [100, 101].

Property	Description
Chemical formula	**$(C_8H_8)_n$**
Glaas Transition temperature (T_g)	**100 °C**
Density	**1.04 g/cm³**
Solubility in water	**Insoluble**
Melting Point	**240 °C**
Boiling point	**430 °C**
Molecular Weight/ Molar Mass	**104.1 g/mol**

3.3.3 Zinc Selenide (ZnSe)

Zinc selenide (ZnSe) is one of the group II-VI semiconductors. ZnSe is particularly interesting for applications related to the interaction with infrared and visible light [102]. Having good mechanical and chemical properties. ZnSe is a cubic structure as shown in figure (3.3) [103]. ZnSe thin films are suitable candidates for semiconductor window layers in the architecture of photovoltaic cells. ZnSe has a large direct band gap of 2.67 eV at room temperature, high optical transmittance and good photosensitivity. Optoelectronic devices based on ZnSe thin films were produced and characterized, such as light emitting diodes [104], solar cells [105], photo detectors [106], transistors [107], and dielectric mirrors [108]. In thin film based solar cells technology, ZnSe is a less toxic alternative to the widely used cadmium sulfide (CdS). Various techniques were used for deposition of ZnSe thin films: chemical bath deposition [109], thermal evaporation (TVE) [110], chemical vapor deposition [111], molecular beam epitaxy or electrodeposition [112]. Table (3-3) explains the most important physical properties of ZnSe [108-109].

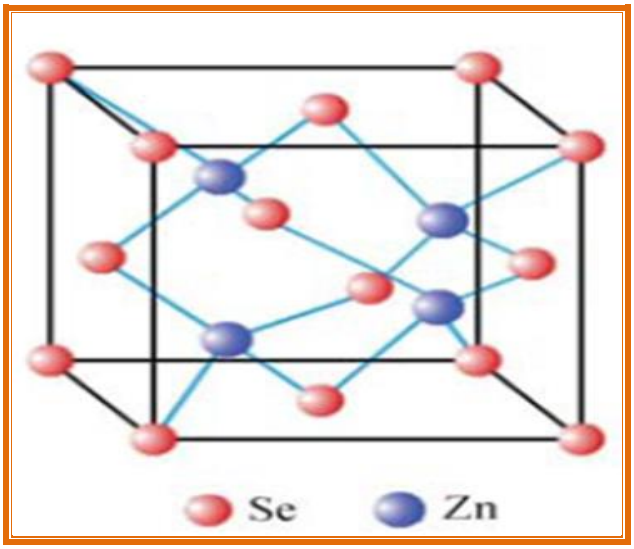

Fig. (3.3): The Chemical Structure of ZnSe [103]

Table (3-3) Physical Properties of ZnSe [108-109]

Property	Description
Chemical formula	ZnSe
Chemical structure	cubic
Energy gap	2.67 eV
Density	5.27 g/cm³
Refractive index	2.403
Melting Point	1525 °C
Thermal conductivity	20 W/mK
Molecular weight Mw (gm/mol)	144.35gm/mol

3.3 Preparation of (PS/PMMA/ZnSe) Nanocomposites films

The following method is used to produce the (PS/PMMA/ZnSe) nanocomposites, as shown in Figure (3.1). The polymer blend was prepared by dissolving 0.5 wt.% of Polystyrene (PS) in 50 ml of chloroform and using a magnetic stirrer for 1/4 hour at room temperature after which it bec ame a homogeneous mixture and then we added 0.5 wt.% of Poly methyl methacrylate (PMMA) with continuous magnetic stirring for one hour until the mixture became homogeneous. The fabricated nanocomposite is prepared by adding the ZnSe NPs to the solution of (PS/PMMA) blend with concentration of 1, 3, and 5 wt. % as shown in Table (3-4). Then it was casted into a glass petri dish and left to dry for four days.

Table (3-4): Weight percentages for (PS/PMMA/ZnSe) nanocomposites.

PS (gm)	PMMA(gm)	ZnSe (gm)
0.5	0.5	0
0.495	0.495	0.01
0.485	0.485	0.03
0.475	0.475	0.05

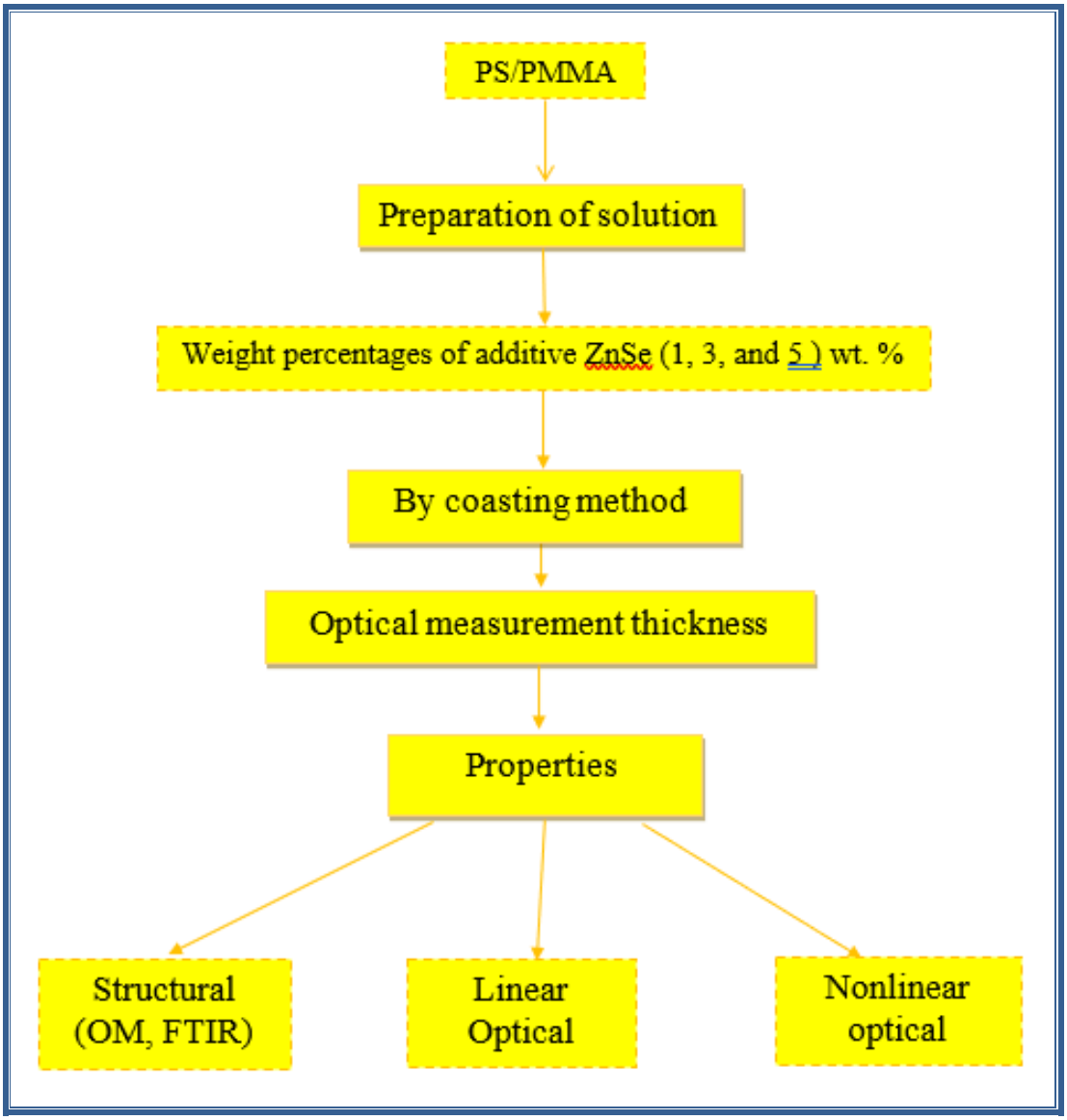

Fig. (3.4): Scheme of Experimental Part

3.4 Optical Measurements of Thickness

Film thickness measurements have been obtained by optical interferometer method. This method is based on interference of the light beam reflection from thin film surface and substrate bottom. He-Ne laser (632 nm) was used and the thickness determined by the difference in optical path lengths of the two reflections, as shown in figure (3.4). The thickness of the prepared of (PS/PMMA/ZnSe) nanocomposites are (0.8, 1.1, 1.3, and 1.5) μm respectively. This work was prepared in (College of Science for Women in Babylon University /department of Laser physics).

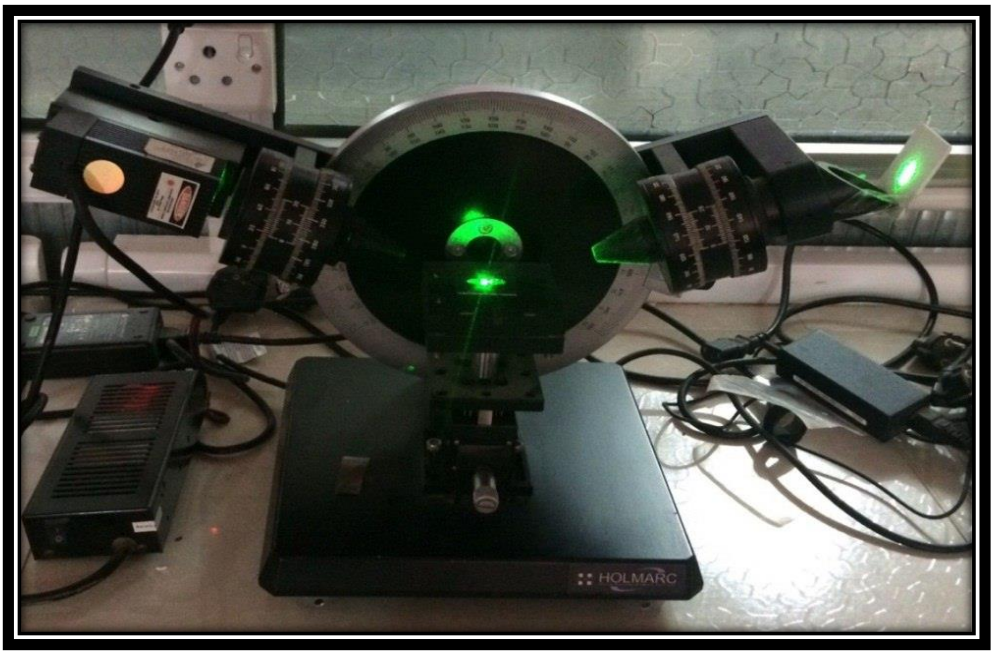

Fig. (3.5) thin film thickness measurement

3.5 Structural Properties for (PS/PMMA/ZnSe) Nanocomposites fims

3.5.1 Optical microscope

The (PS/PMMA/ZnSe) nanocomposite films are analyzed using the optical microscope, which was supplied from Olympus (Top View) type (Nikon-73346), equipped with light intensity automatic controlled camera with magnification

(40x), as shown in figure (3.5). It is implemented in the university of Babylon /college for Pure Science / department of physics.

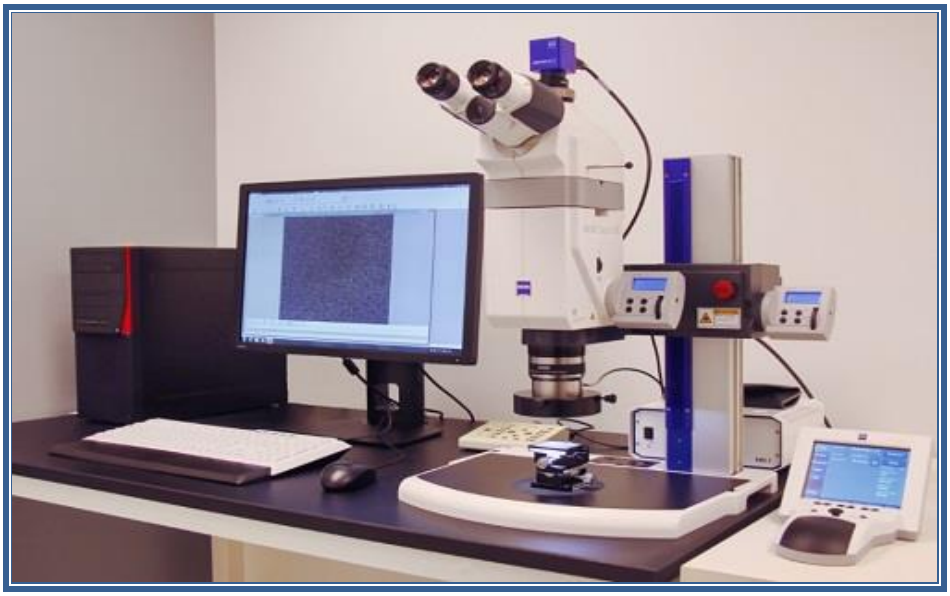

Fig. (3.6): Optical Microscope

3.5.2 Spectral Characterization for FTIR

FTIR spectra were recorded by FTIR Bruker company, German origin, type vertex -70. The spectrum of wave numbers considered is (500-4000) cm^{-1}, as shown in figure (3.6). FTIR has been introduced at the University of Babylon / Education College for Pure Science / Physics.

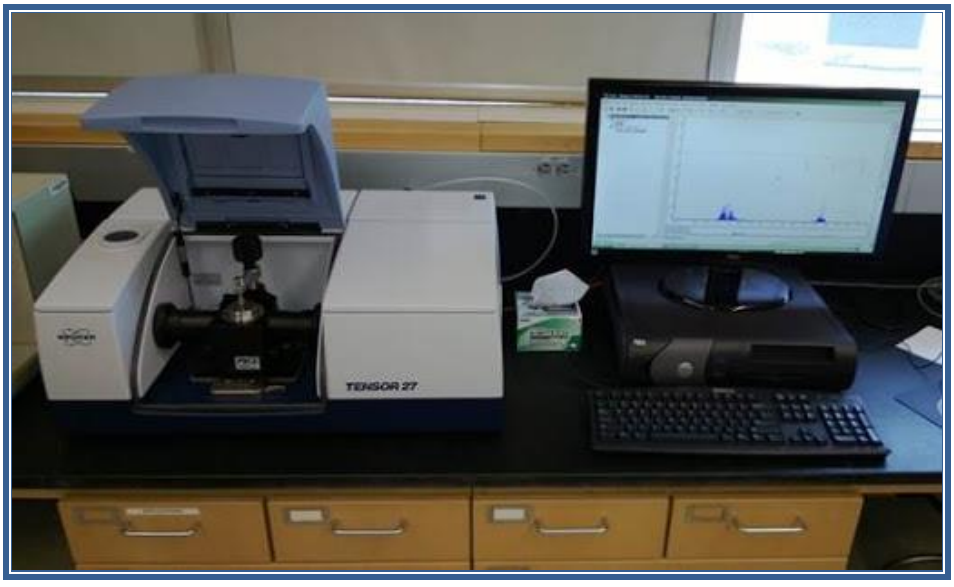

Fig. (3.7): FTIR spectroscopy

3.6 Optical Properties Measurements

The absorption spectra of (PS/PMMA/ZnSe) nanocomposite films were recorded in the wavelength range (200-1100) nm using the double-beam spectrophotometer (Shimadzu, UV-1800 A^0, Japan), as shown in figure (3.7). This device has is located at the University of Babylon / Education College for Pure Science /Physics. The absorption spectrum was recorded at room temperature (RT). To obtain the optical constants, absorbance, transmittance, absorption coefficient, indirect transition, extinction coefficient, refractive index, dielectric constant (real and imaginary parts). A computer program (UV Probe software) was used.

Fig. (3.8): UV Photographic of spectrophotometer

3.7 Nonlinear Optical Properties

Nonlinear optical properties of all samples will be explained in details in the following paragraph:

3.7.1 Z-Scan System

To detect nonlinear optical transmittance, a Z-Scan system was used, the parts of which are shown in the figure (3.8 a,b). This experiment (ZSCAN-VER-8) was equipped by (MAHFANAVAR) company. It consists of:

1- Continuous mode (CW) lasers with different wavelengths.
2- Different optical filters to control the intensity of the laser beam.
3- Optical lenses with different focal lengths (5, 8.5 cm).
4- Laser beam splitter to split the beam.
5- The first detector is located directly beyond the beam splitter and is equipped with a 1 mm hole. This detector is used for detecting the nonlinear refraction.
6- The second detector is equipped with a collecting lens and it used for detecting the nonlinear absorption.
7- Connecting wires to transfer signals from the detectors to a device (Controller), which, in turn, is connected to a computer.

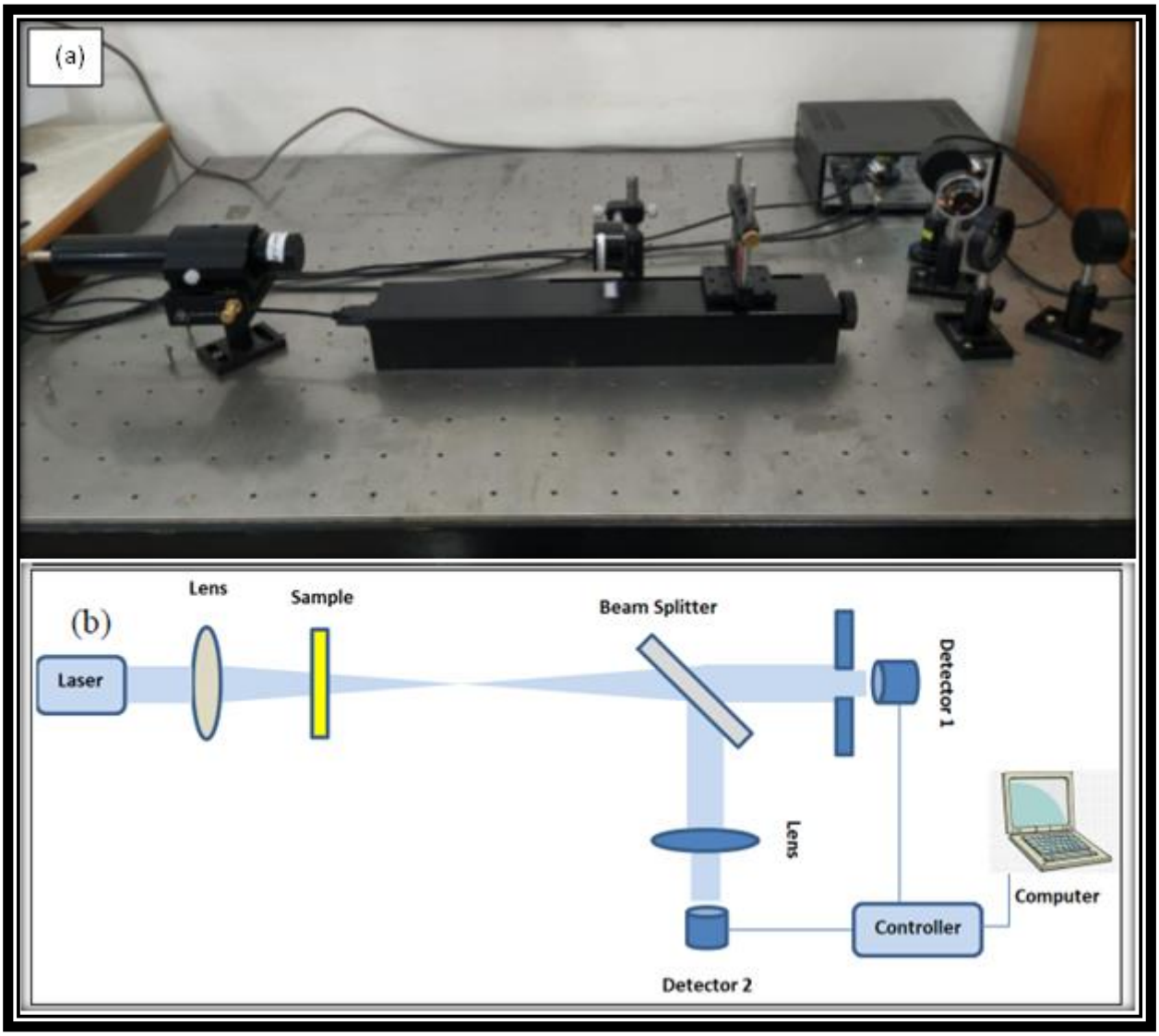

Figure (3.8 a,b) a: demonstrate the Z-Scan technique , b: Schematic diagram and working principle of the technique [110]

Chapter Four

Results and Discussion

4.1 Introduction

This chapter shows the results of the study and the discussion of the results. Structural (optical microscope, Fourier Transform Infrared Spectrometer (FTIR), linear and nonlinear optical measurements of (PS/PMMA/ZnSe) nanocomposites are also discussed in this chapter.

4.2 Structural Properties of (PS/PMMA/ZnSe) Nanocomposites films

4.2.1 The Optical microscope (OM) images

Figure (4.1) presents the images of (PS/PMMA/ZnSe) nanocomposites films taken for samples of variant content at magnification power (10x). The images demonstrate a distinct difference from the samples, as depicted in pictures A, B, C, and D. When the concentration of ZnSe nanoparticles in films composed of polystyrene (PS) and polymethyl methacrylate (PMMA) exceeds 5 wt.%, relatively large size aggregates of nanoparticles are formed within the polymer matrix.

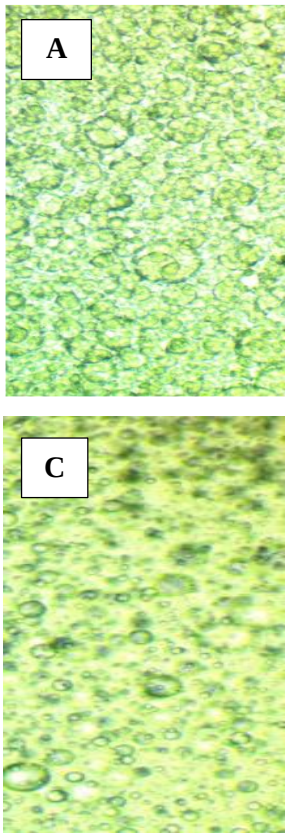

Fig. (4.1): Photomicrographs (10X) for (PS/PMMA/ZnSe) Nanocomposites: (A) for (PS/PMMA) blend, (B) for 1 wt.% ZnSe, (C) for 3 wt.% ZnSe, (D) for 5 wt.% ZnSe

4.2.2 Fourier Transform Infrared Radiation (FTIR) of (PS/PMMA/ZnSe) nanocomposites films

Fourier Transform Infrared Radiation FTIR spectroscopy has been used to analyze the interactions among atoms or ions in (PS/PMMA/ZnSe) nanocomposites. These interactions include changes in the vibrational modes of the nanocomposites. The (FTIR) transmittance spectra of (PS/PMMA/ZnSe) nanocomposites films with the different ratio of (ZnSe) nanoparticles are shown in figure (4.2. A-B-C and D) these spectra are recorded at room temperature in the region (400-4000) cm^{-1}.

From the spectra, the FTIR spectrum of (PS/PMMA) films shows band about 2991.02 cm^{-1} corresponding to the CH_3 bending vibration, and the band 1722.19 cm^{-1} attributed to the C=O stretching vibration. CH_3 stretching vibration is indicated to the band 1447.82 cm^{-1}. The band 1239.92 cm-1 corresponding to the wagging of (CH) The absorption band at 1144.62 attribute to the symmetric

stretching vibration of C-O. The bands 965.60 cm^{-1}, corresponding to the out of plane rings C-H bending, 845.19 cm^{-1} corresponding to the C-C stretching vibrations, 747.87 cm^{-1} corresponding to the stretching vibration. the bands 694.82cm^{-1}, 620.14 cm^{-1} corresponding to the wagging mode of (OH) groups [111]. The FTIR studies show that adding different concentration of ZnSe in images B, C, and D leads to the displacement of some of the bonds and not emergence of new peaks therefore, there is no interaction between ZnSe nanoparticle and the PS/PMMA polymer matrix.

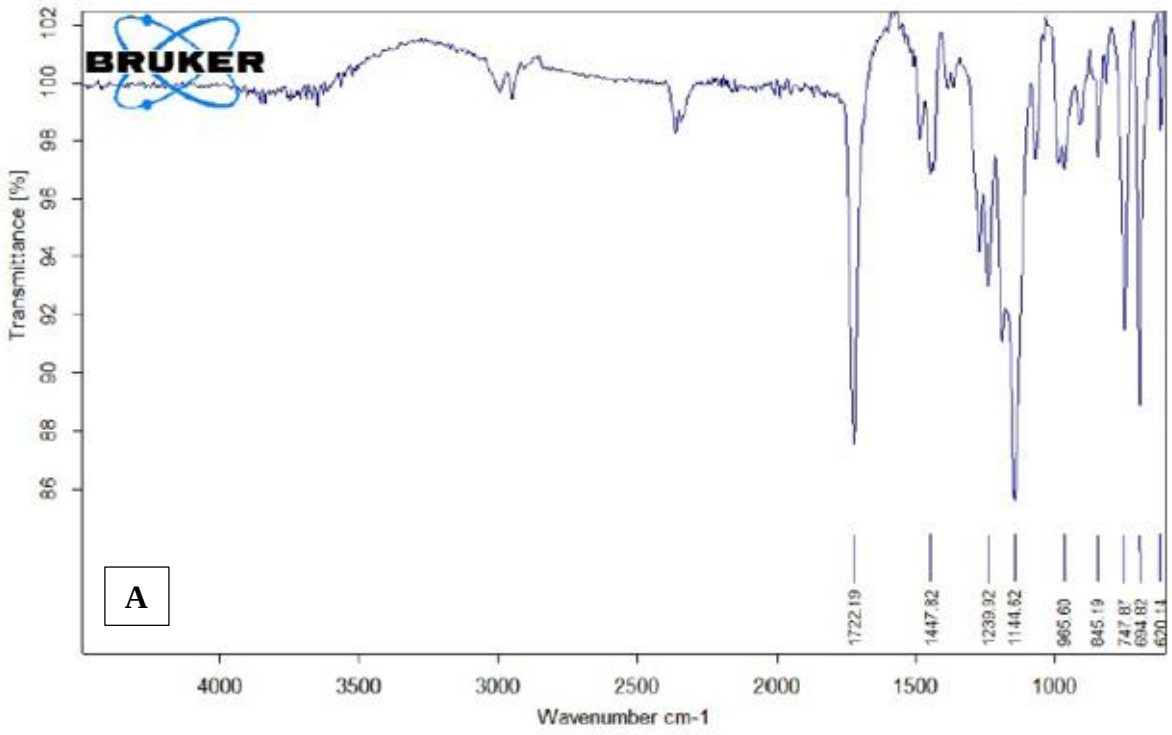
BRUKER
Transmittance [%]
102
100
98
96
94
92
90
88
86
A
1722.19
1447.82
1239.92
1144.52
965.60
845.19
747.87
694.82
620.14
4000
3500
3000
2500
2000
1500
1000
Wavenumber cm-1

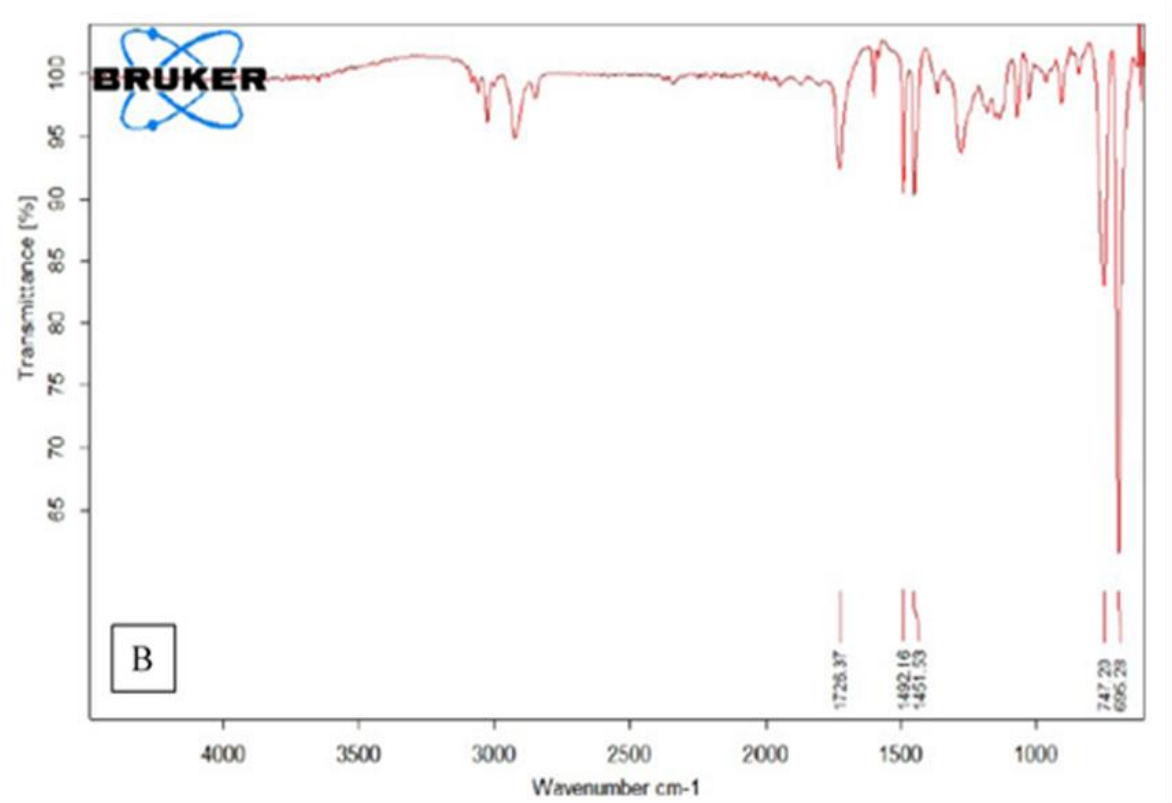
BRUKER
Transmittance [%]
100
95
90
85
80
75
70
65
B
1726.97
1492.16
1451.53
747.29
696.29
4000
3500
3000
2500
2000
1500
1000
Wavenumber cm-1

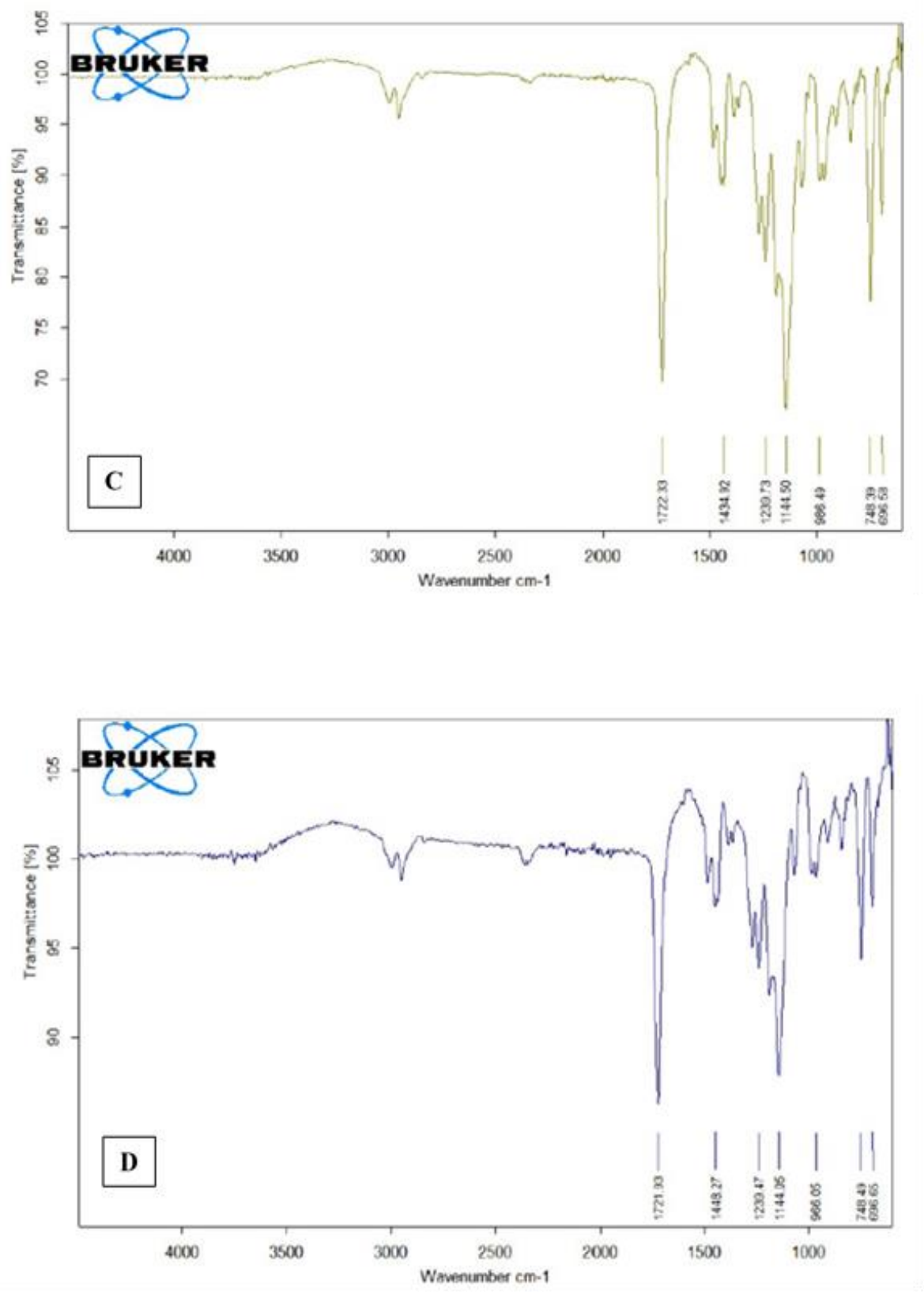

Fig. (4.2): FTIR spectra of (A) for (PS/PMMA), (B) for 1 wt.% ZnSe, (C) for 3 wt.% ZnSe, (D) for 5 wt.% ZnSe

4.3 The Optical Properties

4.3.1 The Absorbance of (PS/PMMA/ZnSe) nanocomposites films

The absorption spectrum of (PS/PMMA/ZnSe) nanocomposites as a function of wavelength of the incident light is depicted in figure (4.3). As it can be seen from the figure, the absorbance of all films is at its maximum at wavelength (260 nm). After that, the absorbance decreases as the wavelength increases. In general, films have a low absorbance in the near infrared and the visible ranges. This can be explained by the following: at long wavelength the incident photon doesn't have enough energy to interact with atoms, thus the photons will be transmitted. When the wavelength decreases (at the neighborhood of the fundamental absorption edge), the interaction between incident photon and material will occur, and then absorbance will increase [110].

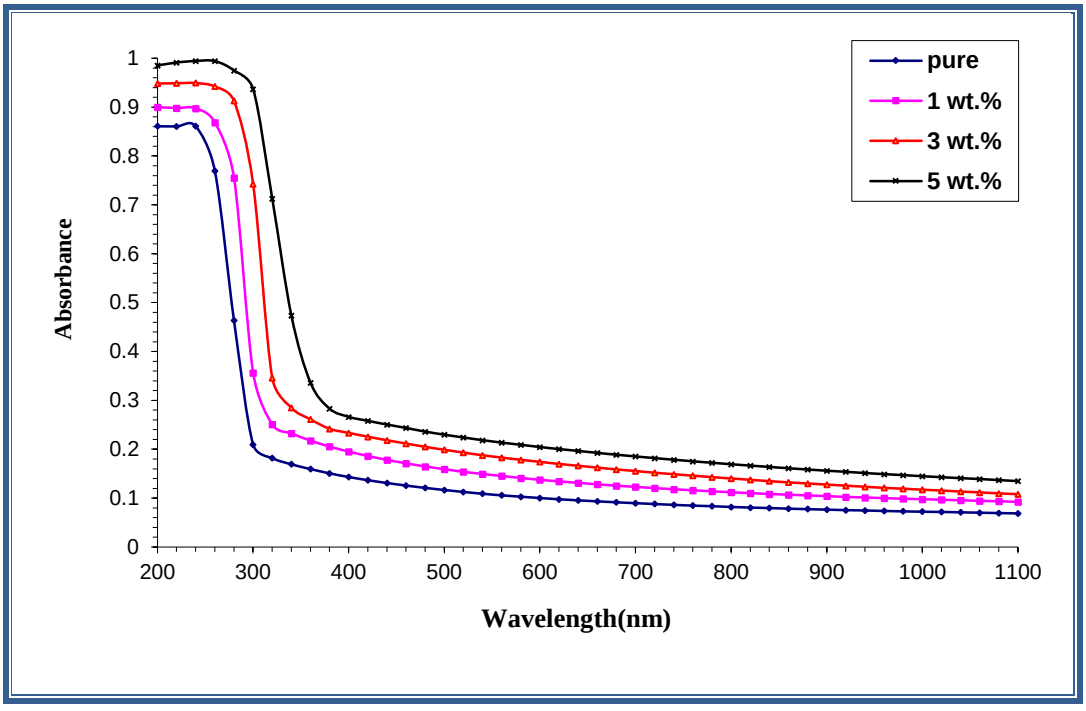

Fig. (4.3): The absorption of (PS/PMMA/ZnSe) nanocomposites films as a function of wavelength for different concentrations of ZnSe.

4.3.2 The Transmittance of (PS/PMMA/ZnSe) Nanocomposites

The optical transmittance spectrum of (PS/PMMA/ZnSe) nanocomposite is shown in figure (4.4) as a function of wavelength of incident light. Figure (4.4) demonstrates that transmittance reduces when the concentration of ZnSe NPs increases, this is due to the addition of ZnSe NPs having electrons in their outer orbits that can absorb the electromagnetic energy of incident light and move to upper energy levels. Or the addition can increase the scattering in the sample. These procedures do not result in the emission of radiation. As a result, a portion of incident ray is absorbed by material and does not pass through it. In addition, pure PS/PMMA films have high transmittance due to the absence of free electrons (i.e. electrons are covalently bound to atoms). This is because the process of breaking the electron's bond and transferring it to the conduction band requires a high energy photon [111].

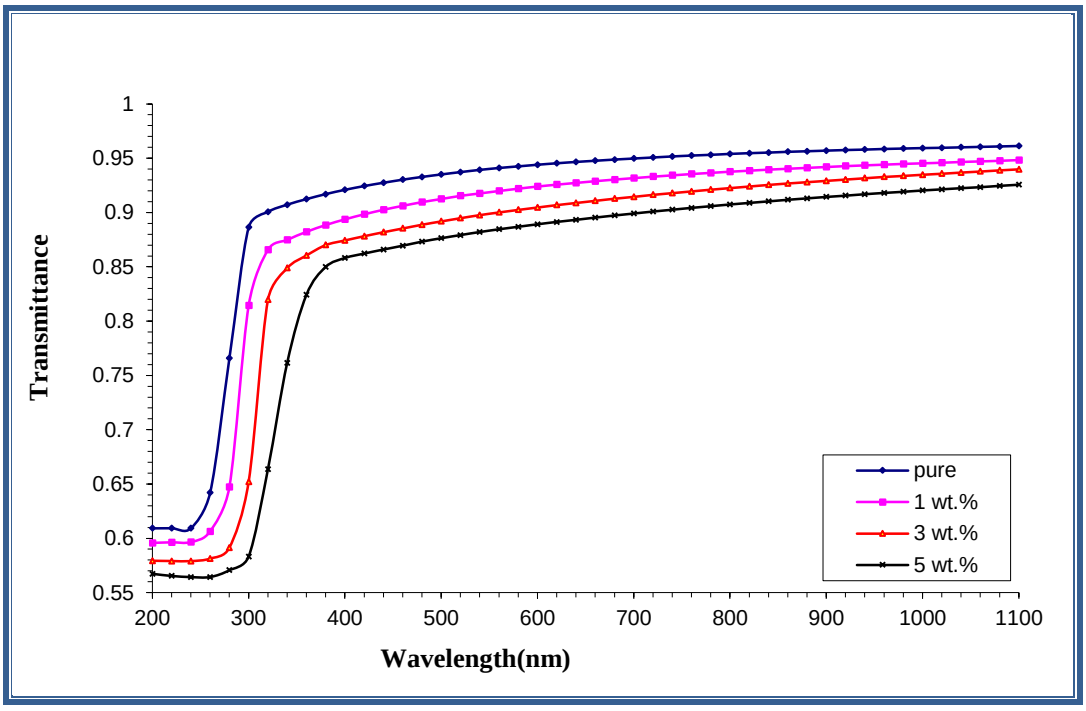

Fig. (4.4): The Relationship between Transmittance of (PS/PMMA/ZnSe) and Wavelength for different concentrations of ZnSe.

4.3.3 Absorption coefficient (α)

The absorption coefficient $(cm)^{-1}$ is found by using the equation (2-5). The absorption coefficient as a function of photon energy for (PS/PMMA/ZnSe) nanocomposites as shown in figure (4.7). The value of the absorption coefficient determines the type of electron transfer. If the absorption coefficient ($\alpha > 10^4$) cm^{-1}, electrons are predicted to undergo a direct transition. However, indirect transition of electrons are expected to occur when the values of the absorption coefficient are lower than (10^4) cm^{-1} [112]. The absorbance coefficient of the (PS/PMMA/ZnSe) nanocomposites is lower than (10^4 cm^{-1}) indicating that the electron transition is indirect.

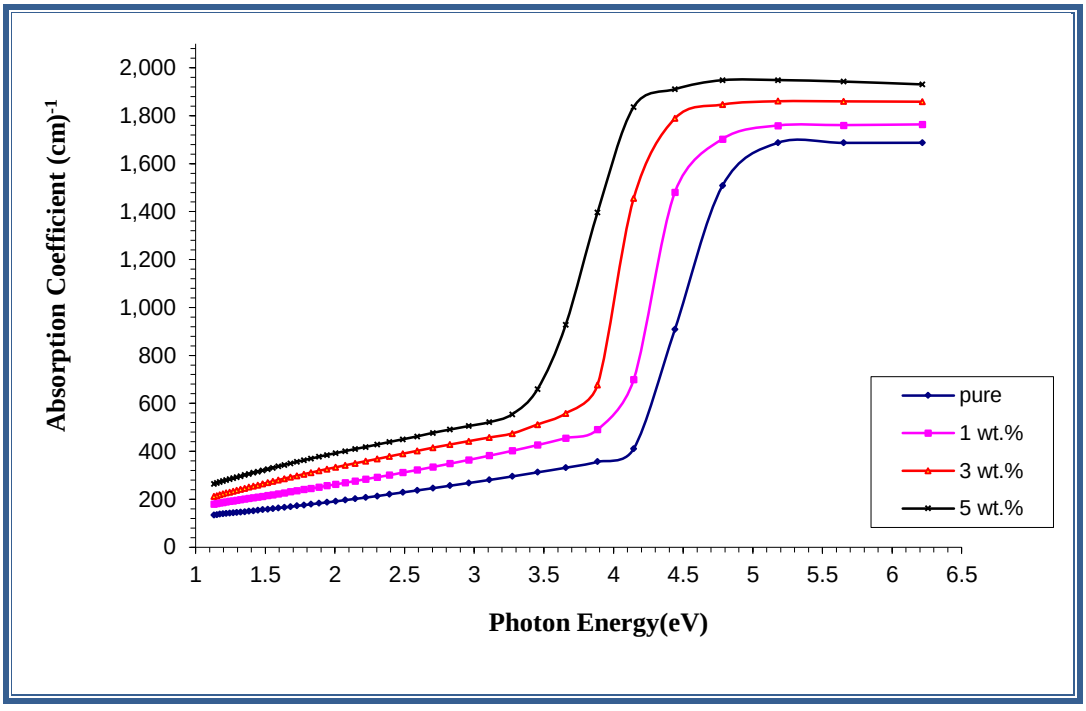

Fig. (4.5): The relationship between the absorption coefficient of (PS/PMMA/ZnSe) and the photon energy for different concentrations of ZnSe.

4.3.4 Energy Gaps of the (allowed and forbidden) Indirect transition

The energy gap for the allowed and forbidden indirect transition bands has been determined using equation (2-9). The variation of the allowed and forbidden indirect energy gap of (PS/PMMA/ZnSe) nanocomposites with the photon energy is depicted in figs. (4.6), (4.7) respectively. the energy gap can be obtained by

the way of drawing a straight line from upper part of the curve towards the x axis. The values obtained are listed in Table (4.1).

The energy gap values are lowered as the concentration of ZnSe NPs increases. This is due to the formation of localized energy levels within the forbidden energy gap, in this situation, the transition occurs in two steps, with the electrons moving from the valence band to the local levels and finally to the conduction band as a result of increasing the concentration of ZnSe NPs. This is related to the heterogeneous nature of nanocomposites with increasing concentrations of (ZnSe) nanoparticles, the density of the localized state increased [113].

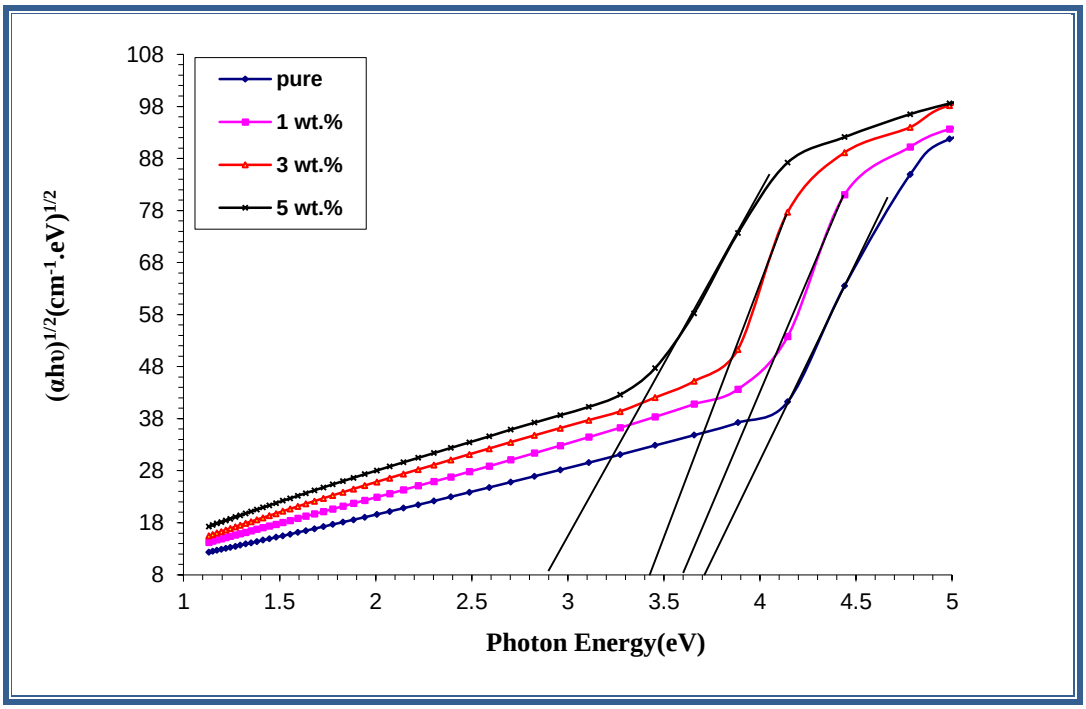

Fig. (4.6): The relationship between $(\alpha h\upsilon)^{1/2}$ $(cm^{-1}.ev)^{1/2}$ and photon energy of (PS/PMMA/ZnSe) nanocomposites for allowed indirect transitions for different concentrations of ZnSe.

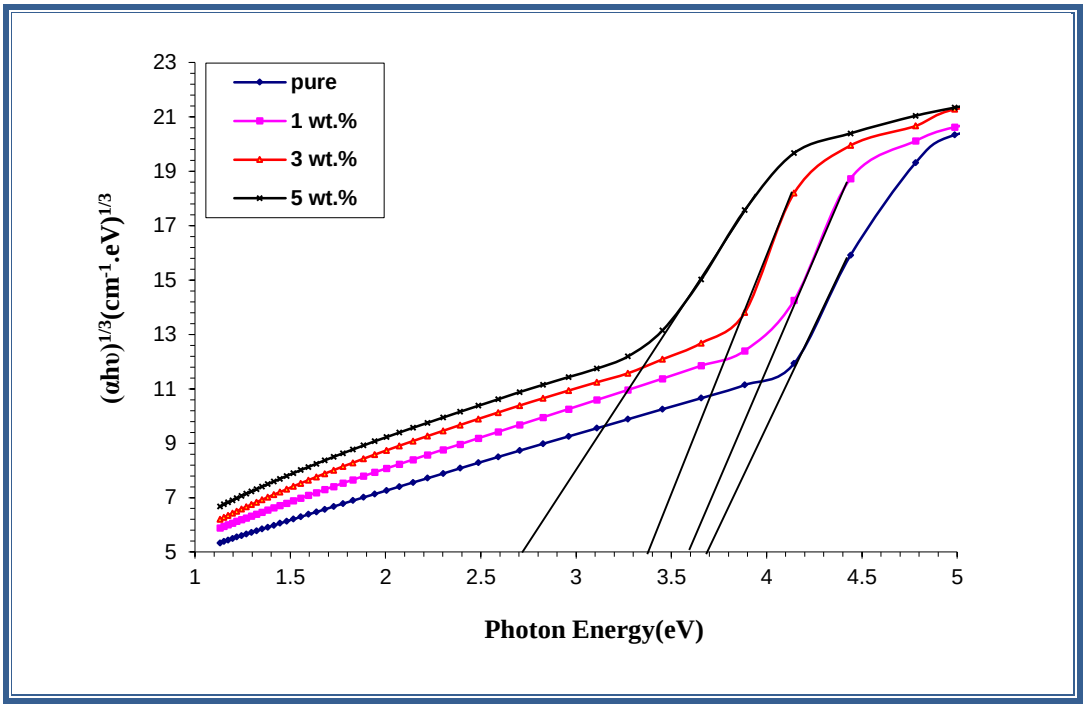

Fig. (4.7): The relationship between $(\alpha h\upsilon)^{1/3}$ $(cm^{-1}.ev)^{1/3}$ and the photons energy of the (PS/PMMA/ZnSe) nanocomposites for the forbidden indirect transition.

Table (4.1): The energy gap for the allowed and forbidden indirect transition for (PS/PMMA/ZnSe) nanocomposites.

ZnSe NPs wt.%	The optical energy gap of the indirect transition (eV)	
	allowed	forbidden
0	3.8	3.7
1	3.51	3.6
3	3.48	3.4
5	2.9	2.7

4.3.5 Refractive Index (n)

The refractive index (n) of a material can be calculated using equation (2-12). Figure (4.8) shows the relationship between the refractive index of (PS/PMMA/ZnSe) nanocomposites and the wavelength. As shown in figure (4.8), the refractive index increases as the weight percentage of (ZnSe) nanoparticles in (PS/PMMA) increases due to the growing density of nanocomposites.

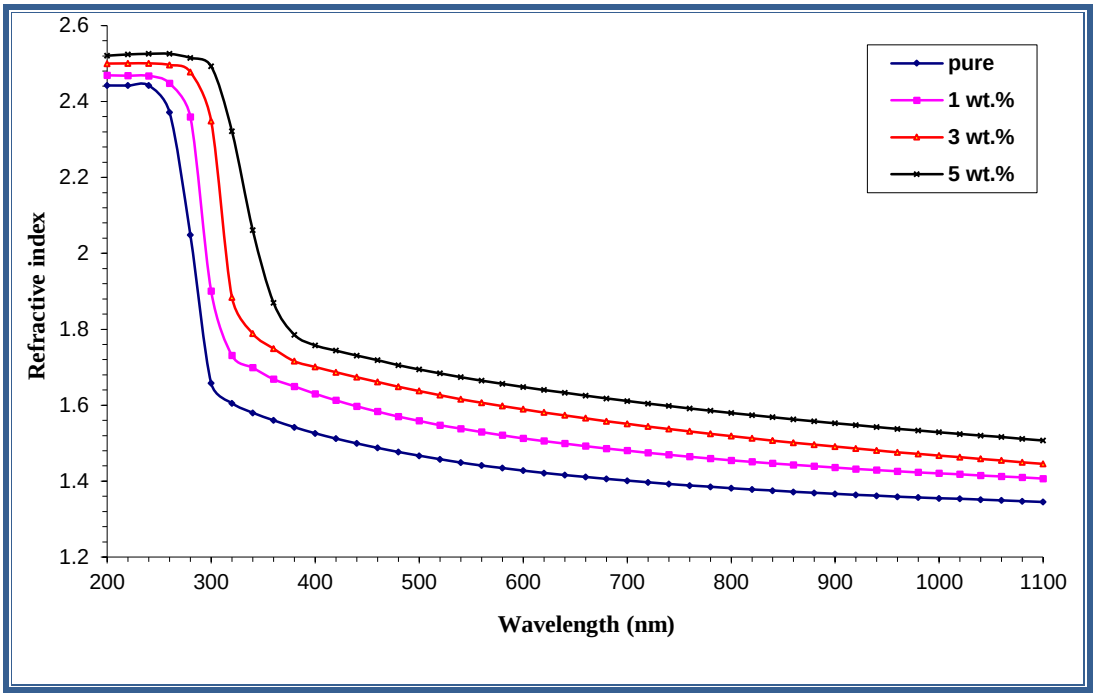

Fig. (4.8). The Relationship between Refractive Index of (PS/PMMA/ZnSe) and Wavelength

4.3.6 Extinction Coefficient (k_0)

Extinction coefficient (k_0) is determined by an equation (2-13). Figure (4.9) shows the relationship between the extinction coefficient of (PS/PMMA/ZnSe) nanocomposites and the wavelength. As can be observed, (k_0) is smaller at low concentrations and increases as the concentration of (ZnSe) nanoparticles increases. This is due to the fact that the absorption coefficient increases as the percentage of (ZnSe) nanoparticles increases. This finding shows that the host polymer's structure will be improved by the atoms of (ZnSe) nanoparticles [114].

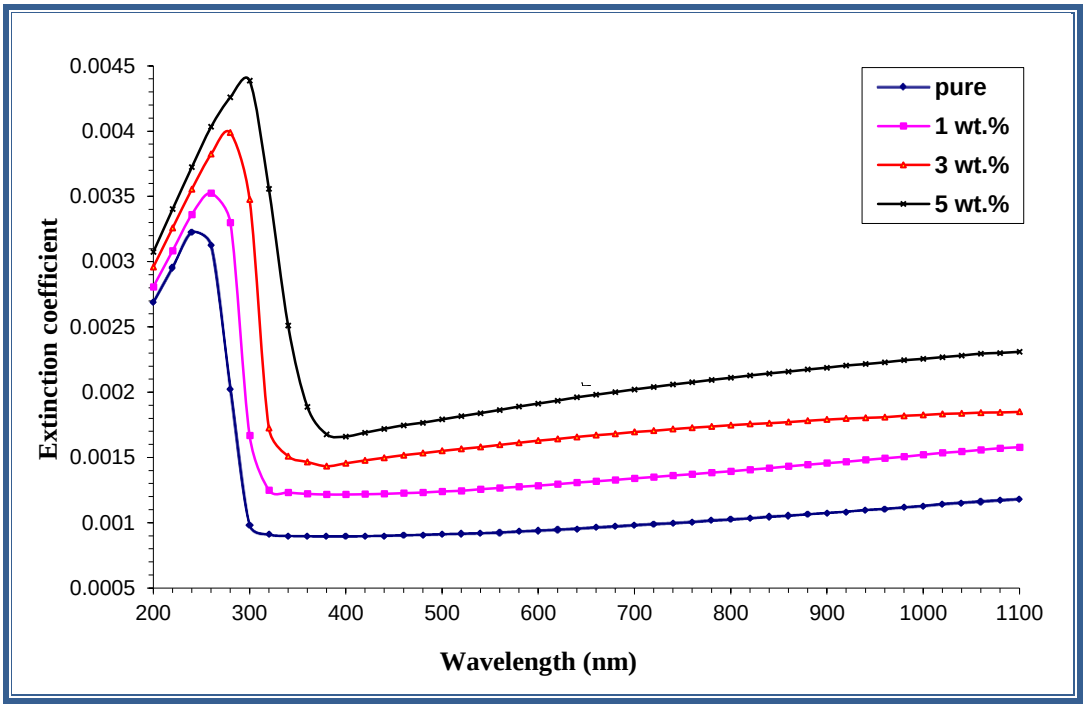

Fig. (4.9): Relationship between extinction coefficient of (PS/PMMA/ZnSe) and wavelength.

4.3.7 The Real and Imaginary Parts of Dielectric Constant (ε_1, and ε_2).

The dielectric constants for two-part (real (ε_1) and imaginary(ε_2)) of (PS/PMMA/ZnSe) nanocomposites were determined using equations (2-14) and (2-15) respectively. Figure (4.10) shows the relationship between (ε_1) and wavelength. As showed in the figure, (ε_1) is strongly dependent on (n) because of the low value of (k^2), the real dielectric constant increases as the concentrations of (ZnSe) nanoparticles increase. Figure (4.11) shows the relationship between (ε_2) and wavelength. As seen in the figure, (ε_2) increased with increasing of concentration of ZnSe NPs which attributed to that (ε_2) is dependent on (k) values, which vary with the absorption coefficient because of the relationship between (k) and (α) [115].

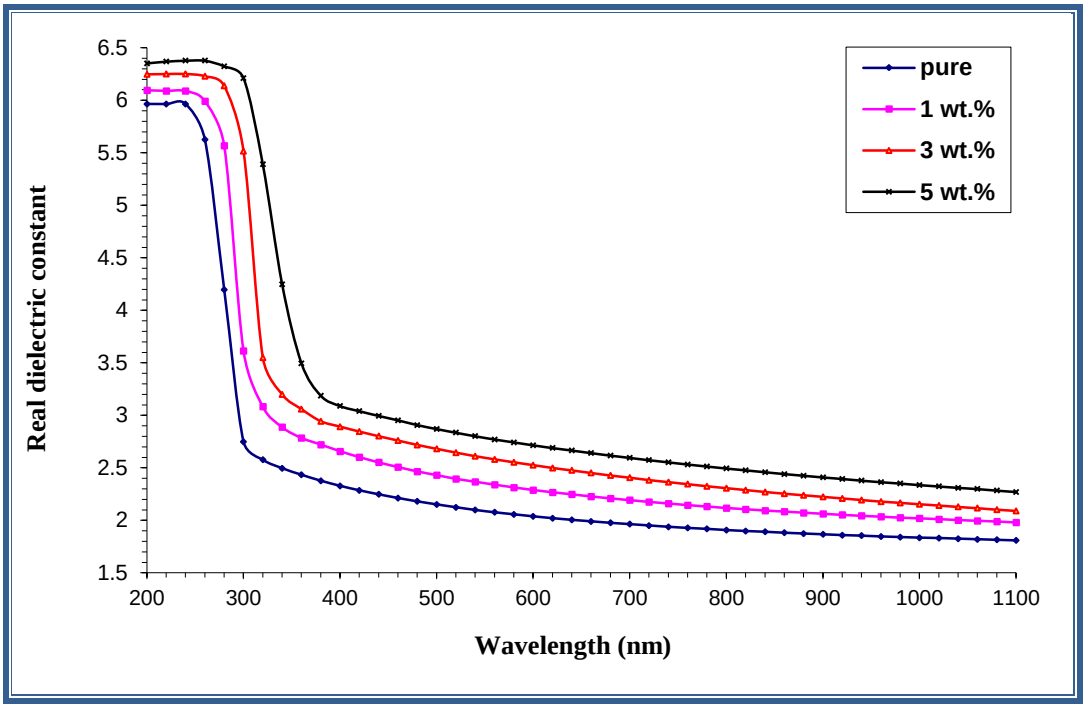

Fig. (4.10): The relationship between the real dielectric constant of (PS/PMMA/ZnSe) and the wavelength.

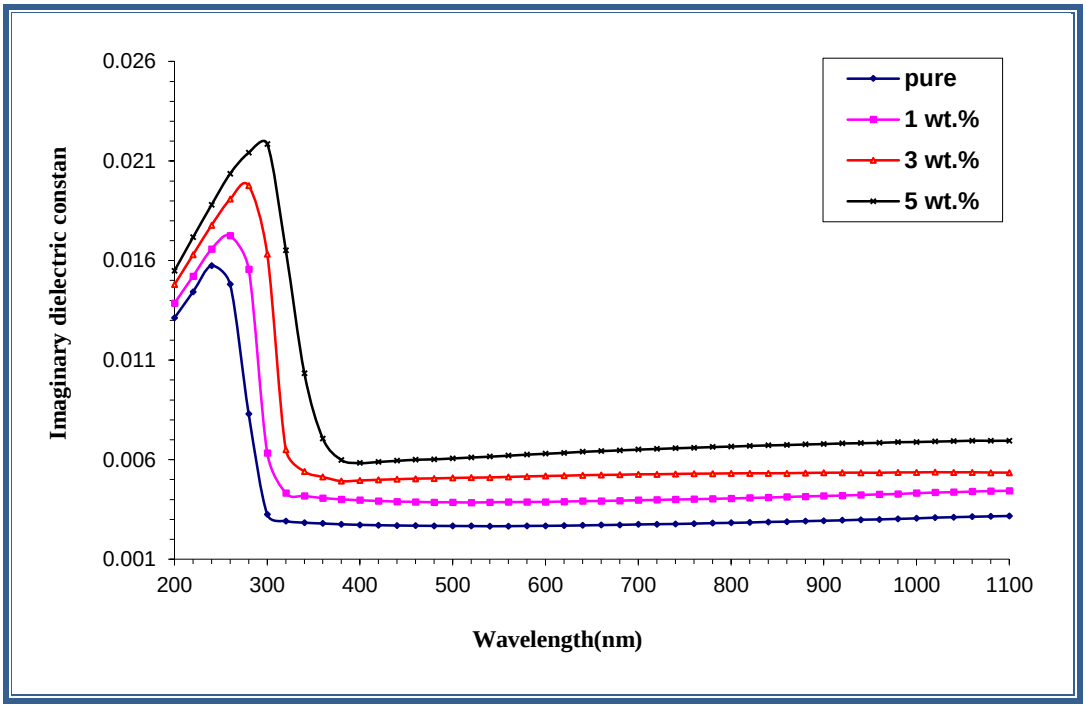

Fig. (4.11): The relationship between the imaginary dielectric constant of (PS/PMMA/ZnSe) and the wavelength.

4.3.8 The optical conductivity

The optical conductivity is determined by equation (2-16). The variation in optical conductivity as a function of wavelength is depicted in figure (4.12). It was discovered that the optical conductivity of (PS/PMMA/ZnSe) increases when the percentages of ZnSe NPs increase to (5 wt.%). As a result of the new levels being created in the band gap, electrons are more easily able to move from the valence band to these local levels and finally the conduction band as a result, the band gap narrows and conductivity increase this conclusion agree with researchers [115].

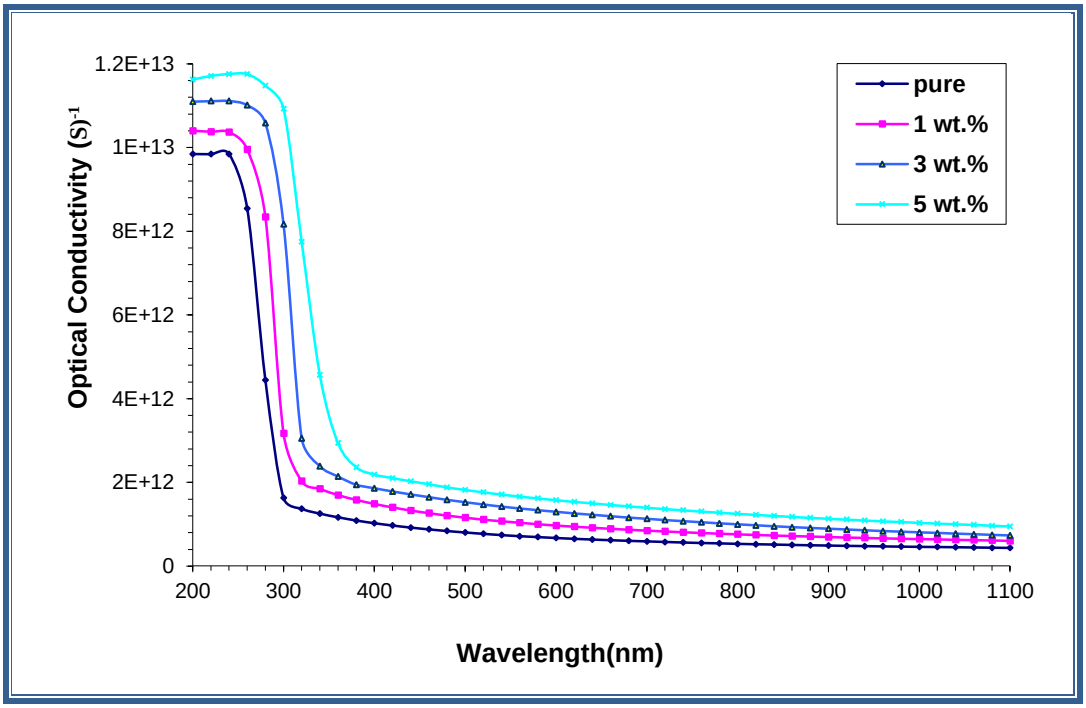

Fig. (4.12): The relationship between optical conductivity of (PS/PMMA/ZnSe) and the wavelength.

4.4. Nonlinear Optical Properties

The nonlinear optical properties of (PS/PMMA/ZnSe) nanocomposite with different concentration (1, 3 and 5 wt.%) of ZnSe NPs using continuous wave (CW) laser at 405 nm wavelength and 20 mW power. Two parts were used to measure the nonlinear properties of the material by Z-Scan technique. The first part is closed-aperture Z-Scan and the second part is the open-aperture Z-Scan.

4.4.1. Closed Aperture Z-Scan of (PS/PMMA/ZnSe) Nanocomposite films

The nonlinear refractive index of the of (PS/PMMA/ZnSe) nanocomposite with different ratios (1, 3 and 5 wt.%) of ZnSe NPs were measured by closed-aperture Z-Scan technique.

The normalized transmittances of Z-Scan measurements as a function of distance are shown in figure (4.13). From this figure, it is observed that the nonlinear effect region is extended from (-65) mm to (65) mm relative to the focus position. The peak followed by a valley transmittance curve obtained from the closed aperture Z-scan data indicates that the sign of the refraction nonlinearity is negative ($n_2<0$), leading to self-defocusing lensing in these samples.

Also, it is obvious that the normalized transmittance decreased with increasing of nano particles weights. This behavior can be attributed to that the nano particles act as a scattering center in the sample, so the increasing of Nano particles consolidates the scattering upon the transmittance of that sample. This result is agreed with previous studies [116].

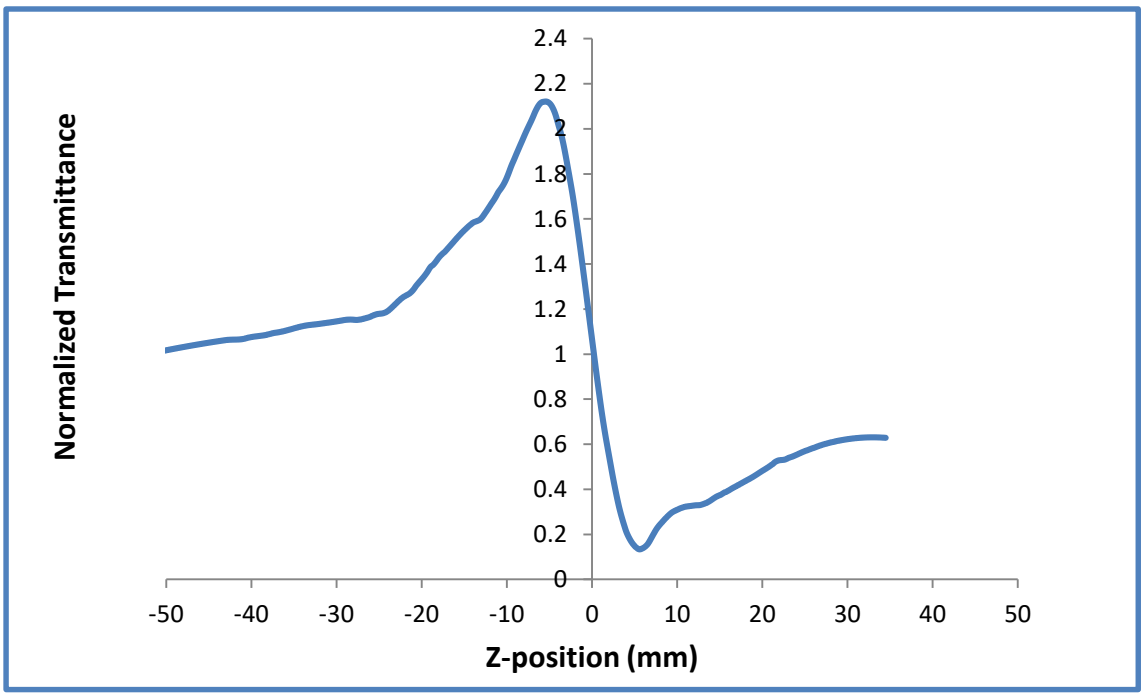
Normalized Transmittance
2.4
2.2
2
1.8
1.6
1.4
1.2
1
0.8
0.6
0.4
0.2
0
-50 -40 -30 -20 -10 0 10 20 30 40 50
Z-position (mm)

(b)

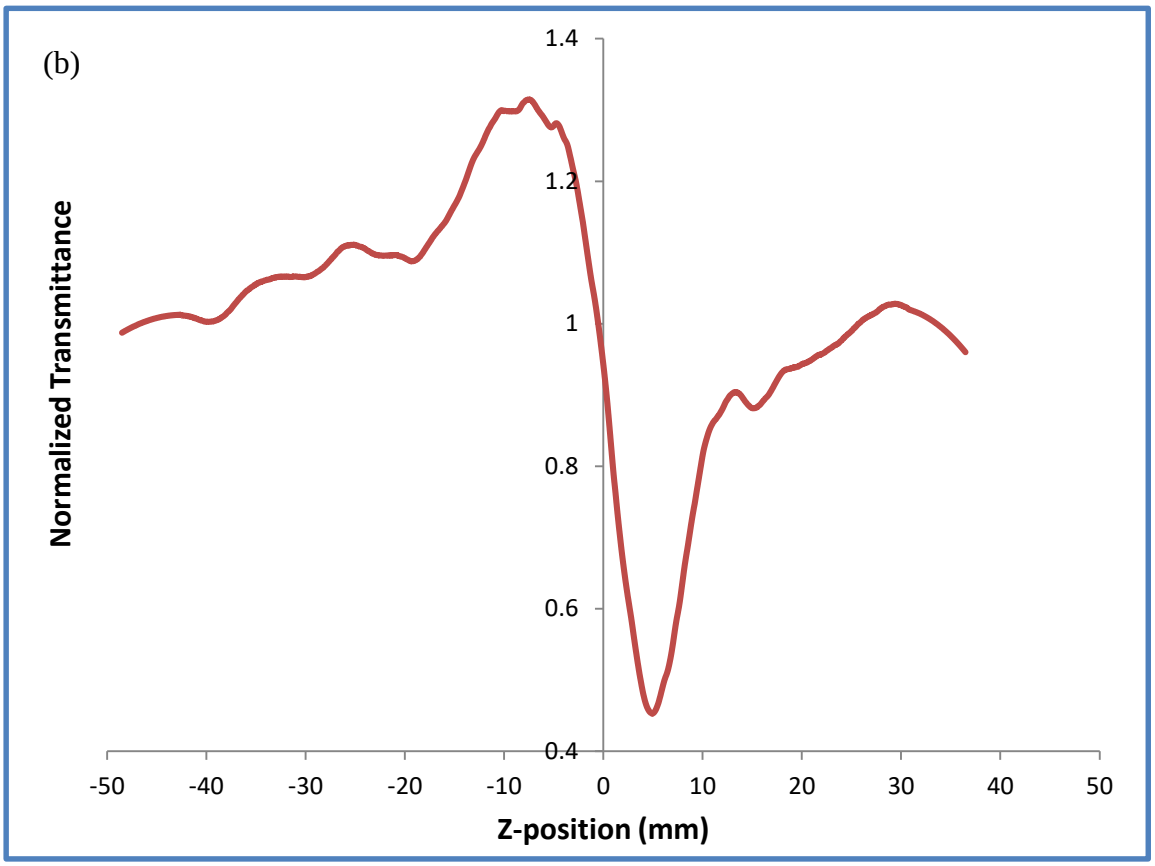
Normalized Transmittance
1.4
1.2
1
0.8
0.6
0.4
-50 -40 -30 -20 -10 0 10 20 30 40 50
Z-position (mm)

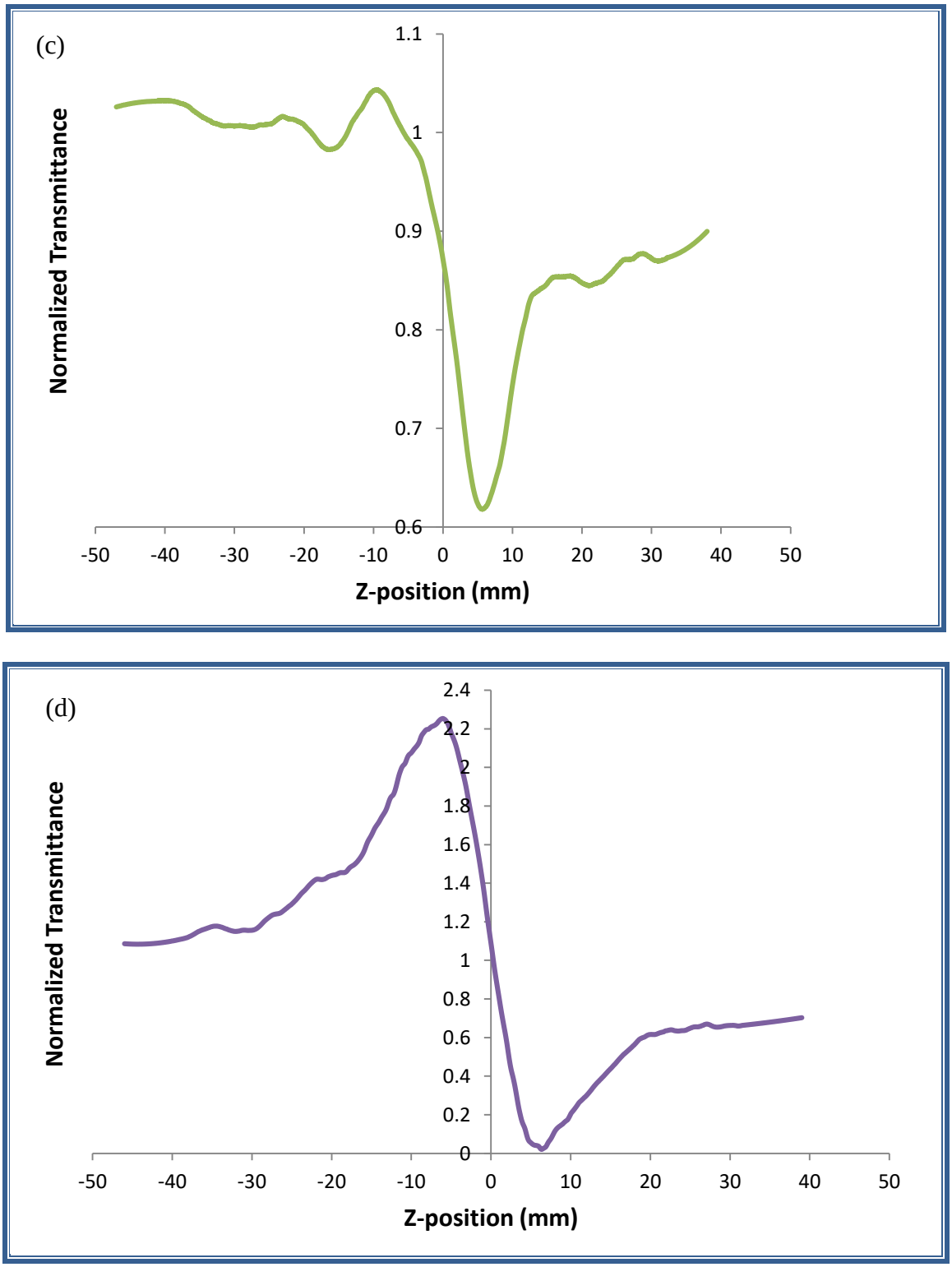

Fig. (4.13): Closed-aperture Z-Scan data for (a) for pure (PS/PMMA), (b) for 1 wt.% ZnSe NPs, (c) for 3 wt.% ZnSe NPs and (d) for 5 wt.% ZnSe NPs

As the sample approaches the beam focus, the intensity increases, resulting in self-lensing within the sample. This self-lensing phenomenon leads to the collimation of the beam onto the aperture in the far field, hence creating an increase in the measured transmittance at the site of the iris. In the event that the beam experiences a nonlinear phase shift while traversing the focal zone due to the sample, the proportion of light reaching the detector will be altered as a consequence of the self-lensing effect created in the material by the high-intensity laser beam. When the sample is translated, the detector will observe a peak and valley in the measured signal.

4.4.2 Opened Aperture Z-Scan of (PS/PMMA/ZnSe) Nanocomposite films

The nonlinear absorption coefficient (β) of (PS/PMMA/ZnSe) nanocomposite with different ratios (1, 3 and 5 wt.%) of ZnSe NPs can be measured by performing the open aperture Z-Scan technique are shown in figure (4.14). The performed open aperture zscan exhibits an increasing in the transmission about the focus of the lens.

Open-aperture Z-Scan of (PS/PMMA/ZnSe) nanocomposite with different ratios (1, 3 and 5 wt.%) of ZnSe NPs were measured by opened-aperture Z-Scan technique. The behavior of transmittance starts linearly at different distances from the far field of the sample position (-Z). At the near field, the transmittance curve begins to decrease until it reaches the minimum value (T_{min}) at the focal point, where Z=0 mm. The transmittance begins to increase towards the linear behavior at the far field of the sample position (+Z). The change of intensity, in this case, is caused by two photon absorption. The photon energy used in this work was about 3.06 eV. Comparing this value with the values of the energy gap of the samples under study proves the possibility of two photons absorption process.

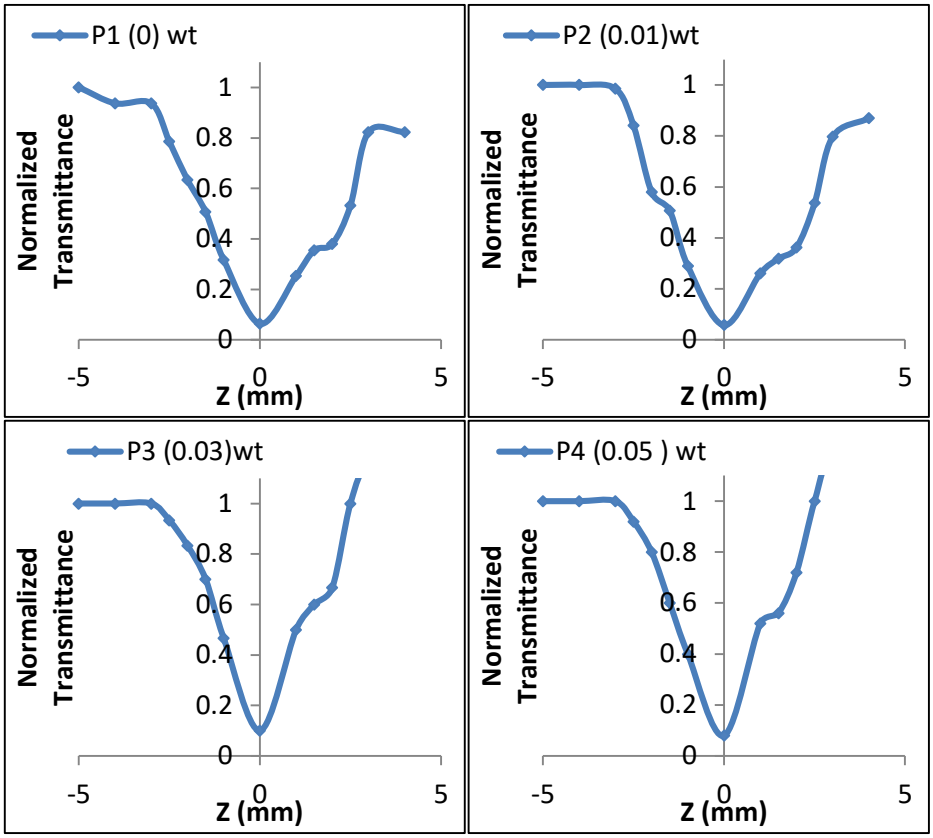

Fig. (4.14): Opened aperture Z-Scan data for pure (PS/PMMA), 1 wt.% ZnSe NPs, 3 wt.% ZnSe NPs, and 5 wt.% ZnSe NPs

Table (4.2) reveals the values of the nonlinear optical parameters for (PS/PMMA/ZnSe) nanocomposites. The Non-linear optical parameters such as transmittance difference (ΔT), nonlinear phase shift ($\Delta \emptyset$), non-linear refractive index (n_2), and nonlinear absorption coefficient have been calculated by using equations of nonlinear refractive index (n_2) and nonlinear absorption coefficient (β), (2-19) and (2-24) respectively. From this table, it can be note that the n_2 and β increase with increasing concentration of ZnSe NPs. This is due to increasing number of molecules per volume unit at high concentrations, as well as nanocomposites have thickness larger than of pure PMMA/PS, which is lead to increasing the nonlinear phase shift. The deviation of the value of (n_2) at concentration of ZnSe of 3% and the value of (β) at concentration of ZnSe of 5% represent measurement errors.

Table (4.2): The values of the nonlinear optical properties for (PS/PMMA/ZnSe) nanocomposites.

λ (nm)	Materials (NPs)	Power (mW)	I_0 (MW/m^2)	L_{eff} (m) $\times10^{-3}$	ΔT	n_2 (m^2/W) $\times10^{-11}$	$\Delta n\times10^{-4}$	β (m/MW)
405	**Pure**	11.2	75.54290833	0.99	2.248815	-0.492	3.71	33.48
	X0.01	1.2	8.09388304	0.996	1.136364	-2.31	1.87	330.51
	X0.03	1.2	8.09388304	0.998	0.555556	-1.13	0.912	396.83
	X0.05	2.66	17.94144073	0.996	2.628205	-2.41	4.32	177.27

4.5 Conclusion

From the obtained results and discussions, the following points are concluded:

1. The optical microscope images show that, at high concentrations, ZnSe nanoparticles form relatively large size aggregates into the polymer matrix.
2. FTIR spectra do not show any new bands as a results of adding ZnSe nanoparticles. This indicates that there is no any kind of interaction between the polymers and the added nanoparticles.
3. The absorption coefficient of (PS/PMMA/ZnSe) nanocomposites increases with the increasing of the concentrations of the (ZnSe) nanoparticles. The absorption coefficient for all films is less than (10^4) cm^{-1}. Refractive index, extinction coefficient, and dielectric constant (real, imaginary) are increasing with the increasing of concentrations of (ZnSe) nanoparticles, while the energy gap for indirect transition (allowed, forbidden) and transmittance decreases with the increasing of the concentrations of (ZnSe) nanoparticles. The optical conductivity increases as the concentrations of (ZnSe NPs) in the (PS/PMMA) increase to (5 wt.%). The films can be used in different electronic device such as solar cells, coatings, photo-detector and microsensors.
4. The absolute value of the nonlinear refractive and the nonlinear absorption coefficient increase with increasing concentration of ZnSe.

4.6 Future works

1. A study on the thermal properties of the (PS/PMMA/ZnSe) nanocomposites.

2. A studying on the mechanical properties of the (PS/PMMA/ZnSe) nanocomposites.

3. Study the optical limiting properties of the samples.

References

Reference

[1] M. Subramanian, “Basics of polymers: fabrication and processing technology”. Momentum Press, (2015).

[2] D. Feldman, “Polymer history,” Des. Monomers Polym., vol. 11, no. 1, pp. 1–15, (2008).

[3] J. McMurry, “Organic chemistry,” Brooks/Cole, USA, vol. 895, p. 1003, (2000).

[4] R. Oslanec, A. C. Costa, R. J. Composto, and P. Vlcek, “Effect of block copolymer adsorption on thin film dewetting kinetics,” Macromolecules, vol. 33, no. 15, pp. 5505–5512, (2000).

[5] F. J. Davis, “Polymer chemistry”: a practical approach. Oxford University Press on Demand, (2004).

[6] G. A. Kontos, A. L. Soulintzis, P. K. Karahaliou, G. C. Psarras, and S. N. Georga, “CA krontiras, and MN Pisanias, Express Polym,” Lett, vol. 1, p. 781, (2007).

[7] S. Hossain, “Optical properties of polymers and their applications,” 2019.

[8] R. Kochetov, “Thermal and electrical properties of nanocomposites, including material properties,” (2012).

[9] D. I. Bower, “An introduction to polymer physics.” American Association of Physics Teachers, (2003).

[10] C. Zweben and C. A. Harper, “Metal matrix composites, ceramic matrix composites, carbon matrix composites and thermally conductive polymers matrix composites,” Handb. Plast. Elastomers Compos., p. 35, (2002).

[11] K.T. Ramesh, "Nanomaterials Mechanics and Mechanisms", The Johns Hopkins University, USA,PP.3, (2009).

[12] D. Liu, W. Wu, Y. Qiu, S. Yang, S. Xiao, Q. Q. Wang, L. Ding, and J. Wang ,"Surface functionalization of ZnO nanotetrapods with photoactive and electro-active organic monolayers", J. of Langmuir, Vol.24, pp.5052-5059, (2008)

[13] T. U. Eindhoven and D. Version, Controlling the rheology of polymer / silica nanocomposites Controlling the rheology of polymer / silica nanocomposites, no. (2010). (2020).

[14] A. H. Doulabi, K. Mequanint, and H. Mohammadi, "Blends and nanocomposite biomaterials for articular cartilage tissue engineering," Materials (Basel)., vol. 7, no. 7, pp. 5327–5355, (2014).

[15] G. A. P. Mariselvi, "Structural, Morphological and Antibacterial Activity of Kaolinite/TiO2 Nanocomposites," J. Nanosci. Technol., vol. 1, no. 1, pp. 16–18, (2015).

[16] P. P. Jeeju, S. Jayalekshmi, K. Chandrasekharan, and P. Sudheesh, "Enhanced linear and nonlinear optical properties of thermally stable ZnO/poly (styrene)–poly (methyl methacrylate) nanocomposite films," Thin Solid Films, vol. 531, pp. 378–384, 2013.

[17] N. G. Hamed and M. Rahem, "To Study the Silver Concentration Effect on the Optical and Electrical Properties of the Ag/PMMA Composites," Eng. Technol. J., vol. 32, no. 1 Part (B) Scientific, 2014.

[18] Tripathi, S. K., & Kaur, R. (2015). Investigation of non-linear optical properties of CdS/PS polymer nanocomposite synthesized by chemical route. Optics Communications, 352, 55-62.

[19] Makki, A. H., AL-Hamadani, A. H., & Husien, M. A. (2016). Dopant Effect on The Nonlinear Optical Properties of TiO2-PMMA Nano Composites for Optical Limiter Applications. Engineering and Technology Journal, 34(5 Part (A) Engineering).

[20] M. T. Ramesan, M. Varghese, and P. Periyat, "Silver-doped zinc oxide as a nanofiller for development of poly (vinyl alcohol)/poly (vinyl pyrrolidone) blend nanocomposites," Adv. Polym. Technol., vol. 37, no. 1, pp. 137–143, 2018.

[21] J. Wang and W. J. Blau, "Inorganic and hybrid nanostructures for optical limiting," J. Opt. A Pure Appl. Opt. Vol.11, PP1–16 (2019).

[22] Alsaad, A. M., Al-Bataineh, Q. M., Ahmad, A. A., Jum'h, I., Alaqtash, N., & Bani-Salameh, A. A. (2020). Optical properties of transparent PMMA-PS/ZnO NPs polymeric nanocomposite films: UV-Shielding applications. Materials Research Express, 6(12), 126446.

[23] Q. M. Al-Bataineh, A. A. Ahmad, A. M. Alsaad, A. D. Telfah, "Optical characterizations of PMMA/metal oxide nanoparticles thin films: bandgap engineering using a novel derived model", Heliyon, Vol. 7, No.1, (2021).

[24] M. H. Noory, Z.A. Hasan, "the Nonlinear Optical Properties for Methylene Blue Dye Doped SiO2 Nanoparticles", MSc., university of Babylon, (2022).

[25] W. Klöpffer, "Infrared Spectroscopy of Polymers," in Introduction to Polymer Spectroscopy, Springer, 1984, pp. 75–107.

[26] C. Mwolfe, N. Holouyak, and G. B. Stillman, "Physical properties of Semiconductor," Printice Hall, New York, 1989.

[27] L. Qian and J. P. Hinestroza, "Application of nanotechnology for high performance textiles," J. Text. apparel, Technol. Manag., vol. 4, no. 1, pp. 1–7, 2004.

[28] G. Attia and M. F. H. Abd El-kader, "Structural, optical and thermal characterization of PVA/2HEC polyblend films," Int. J. Electrochem. Sci, vol. 8, no. 4, pp. 5672–5687, 2013.

[29] S. L. Chuang, "Optical Processes in Semiconductors," Phys. Photonic Devices, 2nd ed.; Boreman, G., Ed, pp. 347–389, 2009.

[30] A. M. Andriesh, M. S. Iovu, and S. D. Shutov, "Chalcogenide non-crystalline semiconductors in optoelectronics," J. Optoelectron. Adv. Mater, vol. 4, no. 3, pp. 631–647, 2002.

[31] C. Kittel, "Introduction to solid state physics," 1976.

[32] J. I. Pankove, Optical processes in semiconductors. Courier Corporation,

1975.

[33] A. Naser M, S. Zaliman, H. Uda, and A.-D. Yarub, “Investigation of the absorption coefficient, refractive index, energy band gap, and film thickness for Al0. 11Ga0. 89N, Al0. 03Ga0. 97N, and GaN by optical transmission method,” 2009.

[34] D. L. Makhija, K. D. Patel, V. M. Pathak, and R. Srivastava, “Optical transitions in WSe2 single crystals,” J. Ovonic Res. Vol, vol. 4, no. 6, pp. 141–145, 2008.

[35] J. I. Pankove, “Optical processes on semiconductors Dover publication,” Inc. New york, 1971.

[36] R. G. Kadhim, “Study of some optical properties of polystyrene-Copper nanocomposite films,” World Sci. News, vol. 30, pp. 14–25, 2016.

[37] C. Mwolfe, N. Holouyak and G. B. Stillman, "Physical properties of semiconductor", prentice Hall, New York, 1989.

[38] **[**H. R. A. AL-Dawodi," A study of the structural and optical properties of obliquely deposited (CdS) thin films", M.Sc. Thesis, University Al-Mustansiriyah, College of Science, 2010.

[39] A. G. Nilens, "deep imparity in semiconductors" , Wiley -Interscience pub., 1973.

[40] J. H. Nahida, “Spectrophotometric analysis for the UV-irradiated (PMMA),” Int. J. Basic Appl. Sci., vol. 12, no. 2, pp. 58–67, 2012.

[41] A. H. Ahmad and A. M. Awatif, “Dopping effect on optical constants of polymethylmethacrylate (PMMA),” Eng. Technol. J., vol. 25, no. 4, 2007.

[42] R. A. Berglund, P. B. Graham, and R. S. Miller, “Applications of in-situ FT-IR in Pharmaceutical Process R&D,” Spectrosc. THEN EUGENE-, vol. 8, p. 31, 1993.

[43] H. Du, G. Q. Xu, W. S. Chin, L. Huang, and W. Ji, “Synthesis, characterization, and nonlinear optical properties of hybridized CdS-polystyrene nanocomposites,” Chem. Mater., Vol. 14, No. 10, pp. 4473–

4479, 2002, doi: 10.1021/cm010622z.

[44] F. L. Rashid, A. Hashim, M. A. Habeeb, S. R. Salman and H. Ahmed, "Preparation of (PS-PMMA) Copolymer and Study The Effect of Sodium Fluoride on Its Optical Properties", Chemistry and Materials Research, Vol.3, No.7. (2013).

[45] Filho, E. L. F. Araujo, C. B. D. and Rodrigues, JR. J. J. 2007. High-order nonlinearities of aqueous colloids containing silver nanoparticles. Journal of the Optical Society of America B, 24(12).

[46] R. Menzel, "Photonics : Linear and Nonlinear Interactions of Laser Light and Matter", 2nd ed., Springer, Berlin, ISBN: 978-3-662-04521-3 , (2001).

[47] M. Papadopoulos, A. Sadlej and J. Leszczynski, "Nonlinear Optical Properties of Matter: From molecules to condensed phases", Springer Netherlands, ISBN 978-1-4020-4850-0, (2006).

[48] R. Boyd, " Nonlinear Optics", 3rd ed., New York ,USA, ISBN: 978-0-12-369470-6, (2008).

[49] R. Boyd and G. Fischer, "Nonlinear Optical Material", Encyclopedia of Materials: Since and Technology, pp.6237-6244, (2001).

[50] I. Khoo, "Liquid Crystals", 2nd ed., A John Wiley and Sons, Inc., Publication, (2007).

[51] R. Philip , G. Kumar , N. Sandhyarani , and T. Pradeep , "Nonlinear Optical Absorption and Induced Thermal Scattering Studies in Organic and Inorganic, Nanostructures", Phys. Rev. Vol.62, No.13160, (2000).

[52] Y. Gun , and H. Chong , "Simple Optical Methods for Measuring Optical Nonlinearities and Rotational Viscosity In Nematic Liquid Crystals", ISBN 978- 953-307- 015-5, pp.111-126 , Vienna, Austria, (2009).

[53] Nemah, S. S., Hasan, Z.A., Influence of Silver Nanoparticles on Optical Properties for (PS-PMMA) Blend, Journal of Global Pharma Technology,11(7), pp325-330,(2019)

[54] Hasan, Z. A., Study the Effect of Magnetic Field on Polymer Doping (

TiO2) Nanoparticles , NeuroQuantology, 17(12) , pp. 39-43,(2019) .

[55] J. H. Nahida, “Spectrophotometric analysis for the UV-irradiated (PMMA),” Int. J. Basic Appl. Sci., Vol. 12, No. 2, pp. 58–67, (2012).Md J. Uddin, B. Chaudhuri, K. Pramanik, T. R. Midday, and B. Chaudhuri," Black tea leaf extract derived Ag nanoparticle-PVA composite film: Structural and dielectric properties", J. Materials science and Engineering B, Vol. 177, No.20, pp.1741- 1747, (2012).

[56] F. L. Rashid, A. Hashim, M. A. Habeeb, S. R. Salman and H. Ahmed, "Preparation of (PS-PMMA) Copolymer and Study The Effect of Sodium Fluoride on Its Optical Properties", Chemistry and Materials Research, Vol.3, No.7. (2013).

[57] Nonlinear Optics 3rd Edition, Robert W. Boyd, 2008

[58] Third order optical nonlinearities by Mansoor Sheik-Bahae, Michael P. Hasselbeck

[59] Filho, E. L. F. Araujo, C. B. D. and Rodrigues, JR. J. J. 2007. High-order nonlinearities of aqueous colloids containing silver nanoparticles. Journal of the Optical Society of America B, 24(12).

[60] Al-Hussainey, A. M., Naser, B. A., Ahmed, R. T., & Abbas, T. M. (2022, November). Non-linear optical properties of azure a organic laser dye. In AIP Conference Proceedings (Vol. 2394, No. 1). AIP Publishing.

[61] A. Ban," Preparation and Study Non-linear Optical Properties of Nematic Liquid Crystal Materials Doped by Nanoparticles", M.Sc. Thesis, University of Babylon, (2016).

[62] Alves, S. Andrea M. Monteiro, Magnus A. Gidlund, AntonioM and Figueiredo Neto, "Thermal-lens effect of native and oxidizedlipoprotein solutions investigated by the Z - Scan technique",International Journal Atheroscler, Vol. 3, No.1, 33-38, (2008).

[63] Mahdi , "Improvement of nonlinear optical properties for mixture Laser

dyes doped PMMA", Iraq J.Laser, part A, 9, 2, pp. 9-14, (2010).

[64] Hassan, Q.M.A. "Third order non linearties and optical limiting properties of rose Bengal at 532 nm wave length" , J. of Basrah Research Science, 33, 2, pp. 76-82, (2007) .

[65] Mao, G. Y. Wu, K. D. Singer," Third harmonic generation in self focused filaments in liquids", Optical Society of America, (2007).

[66] G. A. AL-Dahash, H. N. Najeeb, A. Baqer and R. Tiama, "The Effect of Bismuth Oxide Bi2O3 on Some Optical Properties of Poly vinyl Alcohol", British Journal of Science,Vol.4,pp.117-124, (2012).

[67] G. Svetlana, "Nonlinear Absorption And Refraction of Linearly Polarized Nanoseco nd Laser Radiation by Liquid Crystals In The Transient Regime", Conference on third order nonlinear optical materials, SPIE,Vol.3796, No.277, (1999).

[68] S. Mustafa, "Engineering Chemistry", Library of Arab society for publication and distribution, Jordan, (2008).

[69] R. G. Kadhim, Study of Some Optical Properties of Polystyrene- Copper Nanocomposite Films, World Scientific News, Vol. 30, pp.14-25, (2016).

[70] Nemah, S.S.,Hasan, Z.A., Influence of Silver Nanoparticles on Optical Properties for (PS-PMMA) Blend, Journal of Global Pharma Technology,11(7),pp325-330,(2019)

[71] Hasan Z.A., Study the Effect of Magnetic Field on Polymer Doping (TiO_2) Nanoparticles , NeuroQuantology, 17(12) , pp. 39-43,(2019).

[72] L.W. Tutt and T.F. Boggess, "A review of optical limiting mechanisms and devices using organics, fullerenes, semiconductors and other materials," Prog. Quantum Electron. 17, 299–338 (1993).

[73] L.W. Tutt, A. Kost, "Optical limiting performance of C60 and C70 solutions," Nature 356, 225–226 (1992).

[74] D.J. Hagan, T. Xia, A.A. Said, T.H. Wei, E.W. Van Stryland, "High

dynamic range passive optical limiters," Inter. J. Nonl. Opt. Phys. 2, 483 (1993).

[75] E.W. Van Stryland, S.-B. Mansoor, "Z-scan measurements of optical nonlinearities," in Characterization Techniques and Tabulations for Organic Nonlinear Materials pp. 655– 692, (1998).

[76] D. J.Hagan, E. W. Van Stryland, "Materials for Optical Switches, Isolators, and Limiters", Proceedings of SPIE, SPIE: Bellingham, WA, 1105, 103 (1989).

[77] X.-F. Jiang, L. Polavarapu and S.T. Neo,"Graphene oxides as tunable broadband nonlinear optical materials for femtosecond laser pulses," J. Phys. Chem. Lett. 3, 785–790 (2012).

[78] K. Mansour, M.J. Soileau, and E.W. Van Stryland, "Nonlinear optical properties of carbon-black suspensions (ink)," J. Opt. Soc. Am. B 9, 1100–1109 (1992).

[79] E. Koudoumas and O. Kokkinaki, " Onion-like carbon and diamond nanoparticles for optical limiting," Chem. Phys. Lett. 357, 336–340 (2002).

[80] B. Zhao, B. Cao, W. Zhou, D. Li, W. Zhao, "Nonlinear optical transmission of nanographene and its composites," J. Phys. Chem. C 114, 12517–12523 (2010).

[81] G.-K. Lim and Z.-L. Chen, "Giant broadband nonlinear optical absorption response in dispersed graphene single sheets," Nat. Photonics 5, 554–560 (2011).

[82] K.C. Chin and A. Gohel, , "Modified carbon nanotubes as broadband optical limiting nanomaterials," J. Mater. Res. 21, 2758–2766 (2006).

[83] Y. Chen and Y. Lin, "Carbon nanotube-based functional materials for optical limiting," J. Nanosci. Nanotechnol. 7, 1268–1283 (2007).

[84] R.R. Rishnamurthy and R. alkondan , " Nonlinear characterization of Mercurochrome dye for potential application in optical limiting" , J. Optica

Applicata, Vol. XL, No. 1, (2010).

[85] M.D.Zidan and Z.Ajji , " Optical limiting behavior of disperse red 1 dye doped polymer ", Optics & Laser Technology,Volume 43, Issue 5, Pages 934-937, July (2011).

[86] Fahmi S. Radhi , " Nonlinear responses and optical limiting behavior of 2-Chloro5-nitroanisole dye under CW laser illumination", Journal of Kerbala University , Vol. 10 No.4 , (2012).

[87] Amal F. Jaffar, " Solvent Effect on the Third Order nonlinearity of Oxazine Dye Doped PMMA Films by Using Z-Scan Techniques " , Journal of Advancements in Research & Technology, Volume 2, Issue 11, November-2013 56 ISSN 2278-7763, (2013).

[88] Amal F Jaffar ," Nonlinear Characterization of Rhodamine 610 dye-doped PMMA Thin Films Under 650 nm CW Laser Light Excitation ", Al-Nahrain Journal of Science, Vol 17 No 1, March (2014).

[89] I. Al-Deen H. Al-Saidi and S. Al-Deen Abdulkareem , " Nonlinear optical properties and optical power limiting of Leishman dye using z-scan technique", Journal of Materials Science: Materials in Electronics, Volume 26, Issue 5, pp 2713–2718 , May (2015).

[90] T. A. Osswald, E. Baur, S. Brinkmann, K. Oberbach, and E. Schmachtenberg, “International plastics handbook,” Hanser, Munich, p. 758, 2006.

[91] D. Dorranian, Z. Abedini, A. Hojabri, and M. Ghoranneviss, “Effects of Oxygen RF Plasma on Properties of Poly Methyl Methacrylate Polymer,” J. Theor. Appl. Phys. (IRANIAN Phys. JOURNAL), vol. 2, no. 1, pp. 17–21, 2008.

[92] D. Fischer, Y. Li, B. Ahlemeyer, J. Krieglstein, and T. Kissel, “In vitro cytotoxicity testing of polycations: influence of polymer structure on cell viability and hemolysis,” Biomaterials, vol. 24, no. 7, pp. 1121–1131, 2003.

[93] F. Fixe, M. Dufva, P. Telleman, and C. B. V. Christensen,

"Functionalization of poly (methyl methacrylate)(PMMA) as a substrate for DNA microarrays," Nucleic Acids Res., vol. 32, no. 1, pp. e9–e9, 2004.

[94] R. Çapan, A. K. Ray, A. K. Hassan, and T. Tanrisever, "Poly (methyl methacrylate) films for organic vapour sensing," J. Phys. D. Appl. Phys., vol. 36, no. 9, p. 1115, 2003.

[95] P. Ajayan, L. Schadler and P. Braun, Nanocomposite science and technology Wiley VCH, (2003) .

[96] Malhotra, N., Sheikh, K. and Rani, S. "A Review on Mechanical Characterization of Natural Fiber Reinforced Polymer Composites. Journal of Engineering Research and Studies, 3, 75-80.(2012).

[97] L. L. Zhai, L. GP, W. YW.. (Effect of nano-Al 2 O 3 on adhesion strength of epoxy adhesive and steel) International Journal of Adhesion & Adhesives;28:23 .(2007).

[98] P. Singh ،M .Zhang ،D .Chan (Toughening of a brittle thermosetting polymer: Effects of reinforcement particle size and volume fraction) J. Mater. Sci. 37, 371.((2002

[99] Nagavally, Rahul Reddy."Composite materials-history, types, fabrication techniques,advantages, and applications." Int J Mech Prod Eng 5.9: 82-7(2017).

[100] Wang, B. B. and Xu, X. Z. (2009). "The study of effects of time and temperature on growth of nanocrystalline Zinc Selenide synthesized by hydrothermal method". Journal of Crystal Growth, 311: 4759-4762.

[101] Wang, S., You, J., Geng, B., & Cheng, Z. (2011). Fabrication of ZnSe hexagonal prism with pyramid end through the chemical vapour deposition route. CrystEngComm, 13(2), 668-673.

[102] M. GODLEWSKI, E. GUZIEWICZ, K. KOPALKO, E. LUSAKOWSKA, E. DYNOWSKA, M.M. GODLEWSKI, E.M. GOLDYS, M.R. PHILLIPS, Origin of white color light emission in ALE-grown ZnSe, J Lumin, 102, pp. 455-459, 2003.

[103] A. RUMBERG, C. SOMMERHALTER, M. TOPLAK, A. JAGER-WALDAU, M.C. LUX-STEINER, ZnSe thin films grown by chemical vapour deposition for application as buffer layer in CIGSS solar cells, Thin Solid Films, 361, pp. 172-176, 2000.

[104] B. ULLRICH, Comparison of the photocurrent of ZnSe/InSe/Si and ZnSe/Si heterojunctions, Mater Sci Eng B Solid State Mater Adv Technol, 56, 1, pp. 69-71, 1998.

[105] M.-Y. CHIU, C.-C. CHEN, J.-T. SHEU, K.-H. WEI, An optical programming/electrical erasing memory device: Organic thin film transistors incorporating core/shell CdSe/ZnSe quantum dots and poly(3-hexylthiophene), Org Electron, 10, 5, pp. 769-774, 2009.

[106] L. YAN, J. WOOLLAM, E. FRANKE, Oxygen plasma effects on optical properties of ZnSe films, J Vac Sci Technol, 20, 3, pp. 693-701, 2002.

[107] C. LOKHANDE, P. PATIL, H. TRIBUTSCH, A. ENNAOUI, ZnSe thin films by chemical bath deposition method, Sol Energy Mater Sol Cells, 55, 4, pp. 379-393, 1998.

[108] N. G. Hamed and M. Rahem, “To Study the Silver Concentration Effect on the Optical and Electrical Properties of the Ag/PMMA Composites,” Eng. Technol. J., vol. 32, no. 1 Part (B) Scientific, 2014.

[109] Nemah, S. S., Hasan, Z.A., "Influence of Silver Nanoparticles on Optical Properties for (PS-PMMA) Blend", Journal of Global Pharma Technology,11(7), pp325-330,(2019).

[110] Chapple, P. B., J. Staromlynska, J. A. Hermann, T. J. Mckay, and R. G. McDuff. "Single-beam Z-scan: measurement techniques and analysis." *Journal of Nonlinear Optical Physics & Materials* 6.03: 251-293 (1997).

[111] Hasan, Z. A., "Study the Effect of Magnetic Field on Polymer Doping (TiO2) Nanoparticles" , NeuroQuantology, 17(12) , pp. 39-43,(2019)

[112] H. Neama, N. AL-Khegani, "The Effect of Ferrous Chloride (FeCl2) on Some Optical Properties of Polystyrene", Academic Research

International, Vol. 5, pp. 161-166, (2014).

[113] Md J. Uddin, B. Chaudhuri, K. Pramanik, T. R. Midday, and B. Chaudhuri," Black tea leaf extract derived Ag nanoparticle-PVA composite film: Structural and dielectric properties", J. Materials science and Engineering B, Vol. 177, No.20, pp.1741- 1747, (2012).

[114] T. Beraada and G. al-Adam, " The Updated Chemistry of Large Molecules", University of Basrah, (1989).

[115] AA Ali, ZF Mahdi "Investigation of nonlinear optical properties for laser dyes-doped polymer thin film ", Iraqi journal of physics 10, (19): (54-69), (2012).

[116] G. Svetlana, "Nonlinear Optical Response of Cyanobiphenyl Liquid Crystals to High-Power, Nanosecond Laser Radiation", Journal of Nonlinear Optical Physics & Materials, Vol. 9, No.3, pp. 365-411, (2000).

الخلاصة

في هذه الدراسة، تم تحضير المتراكب النانوي (PS/PMMA/ZnSe) باستخدام طريقة الصب مع نسب وزنية مختلفة من جسيمات ZnSe النانوية (1 و3 و 5) % wt. .

تم تشخيص الخصائص التركيبية والخواص البصرية الخطية واللاخطية للمتراكب النانوي (PS/PMMA/ZnSe). تتضمن الخصائص التركيبية المجهر الضوئي والتحليل الطيفي للأشعة تحت الحمراء (FTIR). أظهرت صور المجهر الضوئي توزيع الجسيمات النانوية ZnSe بشكل تجمعات ذات احجام كبيرة نسبيا عن التركيز (5wt.%). كذلك لم يظهر طيف (FTIR) للمتراكب (PS/PMMA/ZnSe) أي قمم اضافية مقارنة مع الغشاء (PS/PMMA) وهذا يشير بانه لا يوجد تفاعل بين البوليمر والمواد النانوية المضافة. أظهرت نتائج الخصائص البصرية للمتراكب النانوي بأن الامتصاصية، معامل الامتصاص، معامل الانكسار، معامل الخمود، ثابت العزل الحقيقي والخيالي والتوصيلية البصرية تزداد مع زيادة تركيز جسيمات النانوية ZnSe. النفاذية وفجوة الطاقة للانتقال غير مباشر المسموح والممنوع تقل مع زيادة تركيز الجسيمات النانوية ZnSe. (3.8-2.8)eV

كذلك أظهرت الخواص البصرية اللاخطية أن القيم المطلقة لمعامل الانكسار اللاخطي و كذلك معامل الامتصاص اللاخطي يقل مع زيادة تركيز الجسيمات النانوية ZnSe .

جمهورية العراق
وزارة التعليم العالي والبحث العلمي
جامعة بابل
كلية التربية للعلوم الصرفة
قسم الفيزياء

دراسة تأثير المادة النانوية الشبه موصل(ZnSe) على الخصائص البصرية الخطية واللاخطية للخليط البوليمري(PMMA/PS)

رسالة مقدمة

الى كلية التربية للعلوم الصرفة / جامعة بابل

وهي جزء من متطلبات نيل درجة الماجستير في التربية / الفيزياء

أعداد

ابتسام حمزة راضي عبد الحسين

بكالوريوس تربية /فيزياء

جامعة بابل (2004)

بأشراف

أ. د. زيد عبد الزهرة حسن

1445 هـ

2023 م